



TALLINN UNIVERSITY OF TECHNOLOGY  
SCHOOL OF ENGINEERING  
Department of Materials and Environmental Technology

# THE OXYGEN AND CARBON PRODUCTION FROM CO<sub>2</sub> IN MARS CONDITION

## HAPNIKU JA SÜSINIKU TOOTMINE CO<sub>2</sub>-ST MARSI TINGIMUSEL

MASTER THESIS

Student: Sakina Ibrahimova  
Student code: 202376KAYM  
Supervisors: Research Fellow Sander Ratso, PhD,  
Senior Research Fellow Ivar Kruusenberg, PhD

Tallinn 2022

(On the reverse side of title page)

## **AUTHOR'S DECLARATION**

Hereby I declare, that I have written this thesis independently.  
No academic degree has been applied for based on this material. All works, major viewpoints, and data of the other authors used in this thesis have been referenced.

19.05.2022

Author: Sakina Ibrahimova

*/signature /*

Thesis is in accordance with terms and requirements

19.05.2022

Supervisor: Dr Sander Ratso; Dr Ivar Kruusenberg

*/signature/*

Accepted for defence

".....".....20... .

Chairman of theses defence commission: .....

*/name and signature/*

**Department of Materials and Environmental Technology**

**THESIS TASK**

**Student:** Sakina Ibrahimova 202376KAYM

Study programme KAYM, Materials and Processes for Sustainable Energetics

main speciality:

Supervisor(s): Sander Ratso, Fellow researcher +372 56563781

Consultants: .....(name, position)

..... (company, phone, e-mail)

**Thesis topic:**

(in English) THE OXYGEN AND CARBON PRODUCTION FROM CO<sub>2</sub> IN MARS CONDITION

(in Estonian) HAPNIKU JA SÜSINIKU TOOTMINE CO<sub>2</sub>-ST MARSIS TINGIMUSEL

**Thesis main objectives:**

1. Determining the weight loss of three eutectic salt mixtures in different conditions
2. Comparison of the mixtures in terms of stability
3. Performing further characterizations for produced carbon sample

**Thesis tasks and time schedule:**

No	Task description	Deadline
1.	Preparing the mixtures and conducting the experiment	10.02.2022
2.	Analyzing the collected results and drawing conclusions	15.03.2022
3.	Writing the thesis	20.05.2022

**Language:** English **Deadline for submission of thesis: 22.05.2022**

**Student:** Sakina Ibrahimova 19.05.2022

*/signature/*

**Supervisor:** Dr Sander Ratso; Dr Ivar Kruusenberg 19.05.2022

*/signature/*

**Consultant:** ..... ".....".....20....a

*/signature/*

**Head of study programme:** ..... ".....".....20....a

*/signature/*

## Non-exclusive licence for reproduction and publication of a graduation thesis<sup>1</sup>

I am Sakina Ibrahimova

1. grant Tallinn University of Technology free licence (non-exclusive licence) for my thesis

THE OXYGEN AND CARBON PRODUCTION FROM CO<sub>2</sub> IN MARS CONDITION

supervised by Dr Sander Ratso and Dr Ivar Kruusenberg

1.1 to be reproduced for the purposes of preservation and electronic publication of the graduation thesis, incl. to be entered in the digital collection of the library of Tallinn University of Technology until expiry of the term of copyright;

1.2 to be published via the web of Tallinn University of Technology, incl. to be entered in the digital collection of the library of Tallinn University of Technology until expiry of the term of copyright.

2. I am aware that the author also retains the rights specified in clause 1 of the non-exclusive licence.

3. I confirm that granting the non-exclusive licence does not infringe other persons' intellectual property rights, the rights arising from the Personal Data Protection Act or rights arising from other legislation.

19.09.2022

---

<sup>1</sup> The non-exclusive licence is not valid during the validity of access restriction indicated in the student's application for restriction on access to the graduation thesis that has been signed by the school's dean, except in case of the university's right to reproduce the thesis for preservation purposes only. If a graduation thesis is based on the joint creative activity of two or more persons and the co-author(s) has/have not granted, by the set deadline, the student defending his/her graduation thesis consent to reproduce and publish the graduation thesis in compliance with clauses 1.1 and 1.2 of the non-exclusive licence, the non-exclusive license shall not be valid for the period.

# CONTENTS

<b>PREFACE</b> .....	<b>6</b>
List of abbreviations and symbols .....	7
<b>INTRODUCTION</b> .....	<b>8</b>
<b>1. LITERATURE REVIEW AND STUDY OBJECTIVES</b> .....	<b>10</b>
<b>1.1 The need for terraforming of Mars and its challenges</b> .....	<b>10</b>
<b>1.2 The current technologies for oxygen and carbon production</b> .....	<b>13</b>
1.2.1 Sabatier reaction .....	13
1.2.2 Reverse Water-Gas Shift Reaction .....	14
1.2.3 Solid oxide electrolysis .....	16
<b>1.3 MSCC-ET AS A PROMISING TECHNOLOGY</b> .....	<b>20</b>
1.3.1 Fundamentals of Molten salt CO <sub>2</sub> capture and electrochemical transformation (MSCC-ET) .....	20
1.3.2. CO <sub>2</sub> capturing mechanism of the MSCC-ET process .....	22
<b>1.4 MSCC-ET for Mars exploration</b> .....	<b>23</b>
<b>1.5 SUMMARY OF THE LITERATURE REVIEW AND AIM OF THE STUDY</b> .....	<b>25</b>
<b>2. EXPERIMENTAL</b> .....	<b>26</b>
<b>2.1 Preparation of eutectic mixtures</b> .....	<b>26</b>
<b>2.2 Simulation of Mars conditions for MSCC-ET process</b> .....	<b>27</b>
2.2.1 Working principle of the oxygen sensor used in the experiment .....	29
2.2.2 X-ray Diffraction (XRD) .....	30
2.2.3 Scanning electron microscopy (SEM) .....	31
2.2.4. Raman spectroscopy .....	32
<b>3. RESULTS AND DISCUSSION</b> .....	<b>33</b>
<b>3.1 Stability of the studied eutectic salt mixtures in Mars conditions</b> .....	<b>33</b>
<b>3.2 XRD characterization</b> .....	<b>39</b>
<b>3.3 Raman spectra</b> .....	<b>40</b>
<b>3.4 SEM images (with EDX spectra)</b> .....	<b>42</b>
<b>CONCLUSION</b> .....	<b>47</b>
<b>REFERENCES</b> .....	<b>49</b>

## PREFACE

The topic of this thesis was suggested by Dr Sander Ratso, a research fellow at NICPB (National Institute Of Chemical Physics And Biophysics). Most of the work was done at the Laboratory of Energy Technologies in NICPB. For the data analysis parts, I consulted fellow researchers (Dr Kerli Liivand and Erkin Najafli) at the laboratory. I was also assisted by Dr Maarja Grossberg, Mehmet Ender Uslu, and Dr Valdek Mikli from Tallinn University of Technology for the characterization of my sample. Overall, the thesis was supervised by Dr Sander Ratso and Dr Ivar Kruusenberg.

I would like to thank my supervisor for introducing me to his project where I gained valuable research experience. At the same time, I am grateful to all people who guided me through tough times and helped me with their knowledge.

The work was financed by the European Space Agency (ESA) under the ESA OSIP project "Electrochemical splitting of CO<sub>2</sub> for carbon and oxygen production in Mars conditions".

The main focus of this research was to evaluate different eutectic salt mixtures for application as an electrolyte in Mars conditions. The aim was to find out the best candidate for carbon and oxygen production in future Mars missions in terms of electrolyte stability. For this purpose, three different eutectic salt mixtures were prepared and characterized. The characterization studies showed that two of the mixtures (Li<sub>2</sub>CO<sub>3</sub>-Na<sub>2</sub>CO<sub>3</sub> and Li<sub>2</sub>CO<sub>3</sub>-K<sub>2</sub>CO<sub>3</sub>) are promising electrolyte candidates for Mars conditions while Li<sub>2</sub>CO<sub>3</sub>-K<sub>2</sub>CO<sub>3</sub> can be even more suitable as the carbon produced with this mixture was found to be useful for applications such as a fuel cell catalyst support.

Keywords: Carbon and oxygen production, eutectic mixtures, molten salt carbon capture and electrochemical transformation, mars conditions, master thesis.

## List of abbreviations and symbols

MOXIE - Mars Oxygen In-Situ Resource Utilization Experiment

STMD - Space Technology Mission Directorate

MEDA - Mars Environmental Dynamics Analyzer

MSSC-ET - Molten Salt Carbon Capture and Electrochemical Transformation

RWGS - Reverse Water-Gas Shift Reaction

PEM - polymer electrolyte membrane

SOE - solid oxide electrolysis

ISRU - International Space Station as an In-Situ Resource Utilization

TRL - technology readiness level

RWGS - Reverse Water-Gas Shift Reaction

IMISPPS - The Integrated Mars In Situ Propellant Production System

SOE - Solid Oxide Electrolysis

NIR - near-infrared

TGA - thermogravimetric analysis

EDX - energy-dispersive X-ray spectroscopy

XRD - X-ray diffraction

BSE - backscattered electrons

EBS - diffracted backscattered electrons

SEM - The scanning electron microscope

( $I_D$ ) - intensities of the D-band and the G-band ( $I_G$ )

n - order of reflection

$\lambda$  - wavelength of the radiation

d - interplanar spacing

$\theta$  - the incident angle between the x-rays and planes

# INTRODUCTION

The Terraforming of Mars is one of the most discussed topics of the XXI century. But it is quite challenging to develop new technologies in this field due to issues like cost, equipment and so on. Some projects have tried to solve these kinds of challenges and one of these projects is called The Mars Oxygen In-Situ Resource Utilization Experiment also known as MOXIE.

MOXIE's mission on Mars is to show that solid oxide electrolysis can break down the carbon dioxide in the Martian atmosphere into carbon monoxide and oxygen. Carbon monoxide is released into the atmosphere, whereas oxygen is collected and utilized in several ways. MOXIE has already completed two successful runs, producing 5.4 grams of 98 per cent pure oxygen in an hour. Although 5.4 grams is not much, it is enough to provide an astronaut with around 10 minutes of breathable oxygen and to show that the technology works [1].

However, the major drawback of the MOXIE technology is that carbon monoxide produced in electrolysis is emitted into the atmosphere while it could be used for some other application. At the same time, with the operating temperature of 800°C and the pressure of 1 bar, 75% of MOXIE's power is used by the compressor and heater leaving only 12% for oxygen production [2]. That is why there is a need for an alternative technology which does not have such limitations. Currently, there is a promising alternative that can produce various carbon nanomaterials which can be used in a variety of applications in the space industry, including battery and ultracapacitor technologies, conductive and strengthening coatings, polymer formulations, water filters, and so on [3]. This technology is called Molten Salt Carbon Capture and Electrochemical Transformation (MSCC-ET) in which carbonate salt electrolyte is used to break CO<sub>2</sub> molecule into solid carbon and molecular oxygen.

There are different eutectic mixtures of carbonate salts used as an electrolyte for the MSCC-ET process such as Li-Na-K carbonate, Li-K carbonate and Li-Na carbonate mixtures. Although certain general knowledge about these salts exists in the literature, there is a lack of some key research data related to the MSCC-ET. For example, the evaporation rates of chosen electrolytes under simulated Mars conditions must be investigated to find the most suitable eutectic mixture for the given conditions.

In this work, Mars conditions were imitated in a laboratory-made reactor set up to run the reaction in three different steps. For the first step, each salt mixture was melted under

Argon flow to understand the decay rate in the neutral state without any CO<sub>2</sub> presence. As the next step, the same salt mixtures were melted under a simulated Martian atmosphere (CO<sub>2</sub>, N<sub>2</sub> and Ar). Finally, the electrodes were placed in the electrolyte to produce carbon and oxygen for further characterization.

# **1. LITERATURE REVIEW AND STUDY OBJECTIVES**

## **1.1 The need for terraforming of Mars and its challenges**

The desire to find and colonize uninhabited areas has always been part of the human nature. This has encouraged homo sapiens to create tools that would help to survive in extreme environments and conditions. At the same time, the need to travel over long distances has led to the invention of transportation vehicles which in turn made it possible to populate very far places in the planet.

The Earth is roughly 4.5 billion years old and during the early development stages of the solar system, our planet's atmosphere would have been unbreathable, containing only nitrogen and carbon dioxide and no oxygen. The earliest life appeared in that period, around 3.7 billion years ago, most likely in the oceans. Archeobacteria and other kinds of life that followed began to use the massive amounts of carbon dioxide in the atmosphere to produce oxygen. This gradually changed the composition of the planetary atmosphere, allowing it to host forms of life that breathe oxygen, including humans. It can be said that the first planet to be terraformed was Earth itself [4].

However, some of the technologies that make our life easier also lead to serious issues that need to be solved without delay. Perhaps, climate change with its terrible repercussions and costly unfavorable effects may be the most urgent problem that humanity has ever faced. It is expected that by 2030, we will already breach the goal of keeping the temperature rise below 1.5°C at pre-industrial levels set in the Paris agreement due to the "accelerated warming" (see Fig.1.1) of the Earth [5]. Such alarming news about the future of our planet makes humanity think about alternatives and often scientists focus on Mars as a viable option.

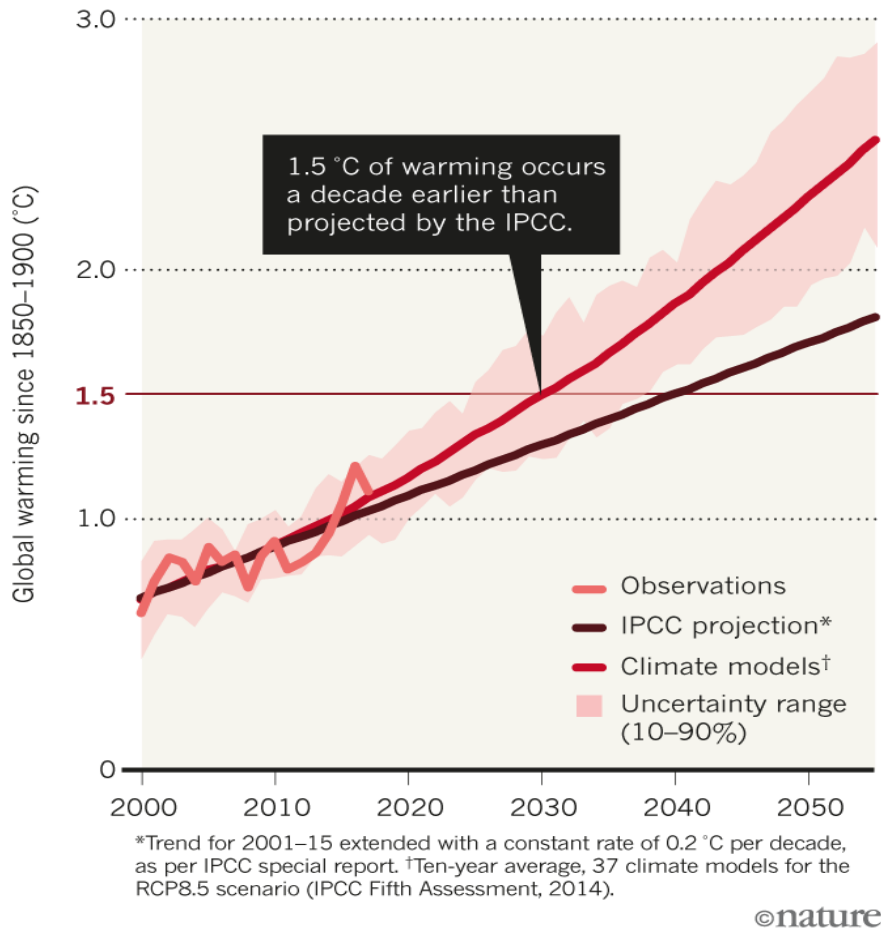


**Figure 1.1** Climate simulations predict that global warming will rise exponentially if emissions go unchecked

Mars is attracting attention for a variety of practical, scientific, and strategic reasons. Mars is the most reachable planet in the Solar System in terms of practicality [6]. It is, after Venus, the second-closest planet to Earth, with a distance between the furthest and closest places in its orbit averaging roughly 360 million kilometres. There are a lot of similarities between Earth and Mars. Both planets, for example, spin at the same velocity and have the same tilt angle. On Earth, a day is 24 hours long, while on Mars, it is 24 hours and 37 minutes long and a year is 365 days long on Earth, but on Mars, it is 687 days long. The Earth's axis tilts at 23.5 degrees, while Mars tilts slightly more at 25.2 degrees. The former orbits at 30 kilometres per second, whereas the latter orbits at 24 kilometres per second. From a scientific standpoint, it is worth mentioning that investigating Mars offers the potential to answer questions about the origin and evolution of life, as well as provide a future destination for human existence. On July 15, 1965, the US Mariner 4 spacecraft made the first successful approach to the red planet and took the first photos of Mars ever sent back to Earth. (Figure 1.2) [7]

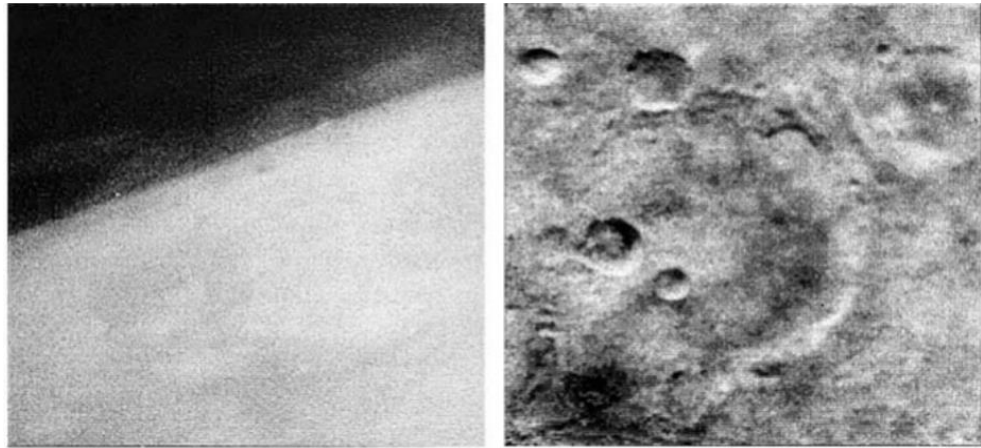


**Figure 1.2.** Mariner 4 images, (a) first ever image of Mars taken at the limb of the planet revealing high clouds, (b) image no. 11, showing large craters on the surface, famous for dashing hopes of a living planet

In the case of Mars, the term 'terraforming' refers to the process of altering the Martian environment to make it more conducive to the existence of terrestrial life [8]. There are three main aspects of terraforming that need to be advanced[4] :

- Scientific-technological aspects. Terraforming is a highly interdisciplinary endeavour including physics, chemistry, and biology, as well as electronics, material science, nanotechnology, and other disciplines. Thus, significant breakthroughs are required in these fields to satisfy the scientific-technological aspects of terraforming.
- Ethical aspects. All technologies have a significant impact on the environment and people's way of life, so there is a need to understand the ethical aspects of terraforming before taking any important steps.
- Financial aspects. As terraforming is a huge financial undertaking, there is a need for a detailed plan that can cover centuries of work.

Although there are important similarities between the environments of Mars and the Earth certain key differences create challenges that need to be solved to make Mars habitable. Scientific-technological terraforming of Mars can be achieved by tackling several major obstacles such as warming the planet, thickening its atmosphere, activating its hydrosphere and producing enough oxygen to make it a habitable place [9]. It can be argued that efficient and large-scale oxygen production is the most difficult among these tasks and significant technological progress needs to be made before it becomes economically and practically viable.

## 1.2 The current technologies for oxygen and carbon production

While the CO<sub>2</sub>-rich atmosphere of Mars is an issue on its own, it can also be considered an opportunity for tandem oxygen and carbon production. Due to the ever-increasing level of CO<sub>2</sub> in our atmosphere, carbon capture and conversion have gotten a lot of scientific interest in the previous two decades and there are mature technologies used in the field. For instance, the Sabatier or Reverse Water-Gas Shift Reactions (RWGS), both of which are used alongside polymer electrolyte membrane (PEM)-based water electrolysis, solid oxide electrolysis (SOE), and the MSCC-ET process, are the key technologies that have emerged for direct CO<sub>2</sub> capture and transformation that can also be relevant in Mars conditions [10] [11] [12]. All of these procedures rely on (electro)chemistry that has been known to split CO<sub>2</sub> for hundreds of years, but they are significantly different in terms of what and how much they can produce.

### 1.2.1 Sabatier reaction

The Sabatier (or methanation) process for CO<sub>2</sub> capture and transformation is based on the exothermic reaction discovered by Paul Sabatier and Jean-Baptiste Senderens:



The process is already in use on the International Space Station as an In-Situ Resource Utilization (ISRU) method in combination with water electrolysis in which electricity is applied to water to produce oxygen (for breathing) and hydrogen:



After the astronauts' carbonate oxygen through breathing, it is again joined with two extra hydrogen molecules via reaction (1.1) to reproduce the original two water molecules and methane, which is then vented [13][14] or pyrolyzed to make carbon or CO with an additional energy cost. The Sabatier process has several advantages, including a high space technology readiness level (TRL), the ability to reclaim methane on Mars for heat generation or the production of higher carbon molecules, and high selectivity (Ni and Ru

catalysts have shown more than 95% conversion and 99% selectivity in multichannel microreactors) [14] [15]. The Sabatier reactors (see Fig. 1.3) are rather simple with basic units comprised of tubes filled with catalysts.

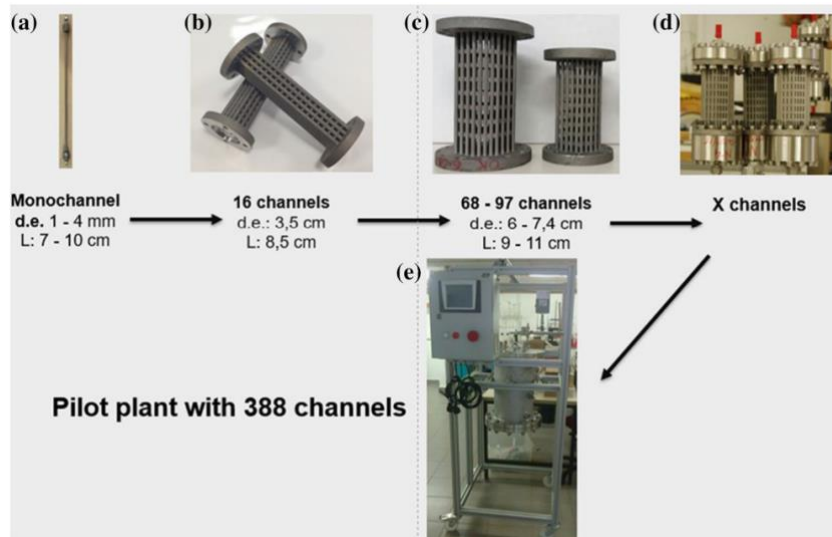


**Figure 1.3.** Sabatier reactors in various scales were developed by Tecnalia [9]

However, there are certain disadvantages including the fact that the reaction is exothermic, necessitating cooling, as well as the high pressure required (15-25 bar), which would require a large compressor and energy budget to power it, as well as the requirement for hydrogen to be continuously added to the process, implying that the hydrogen used for the process would either have to be brought with the mission from Earth or created from mined water on Mars [10], [14], [15].

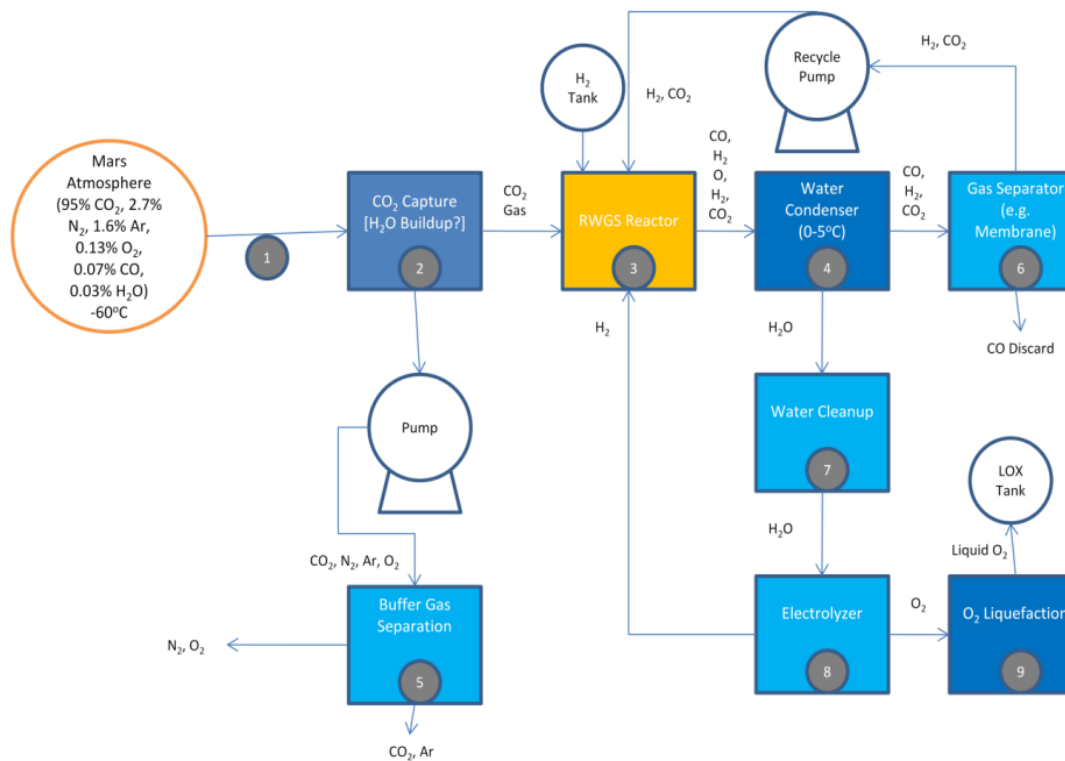
### 1.2.2 Reverse Water-Gas Shift Reaction

The **Reverse Water-Gas Shift Reaction (RWGS)** is based on the following reaction:



This can also be used in combination with water electrolysis (1.2), to produce carbon monoxide and oxygen simultaneously. The RWGS reactor is similar to the Sabatier reactor as it requires a catalyst as well. Due to the presence of a catalyst in the reactor, the reaction can be vulnerable to poisoning caused by additives from the reactant stream and gradual degradation of the catalyst used. Unless run at high pressures (more than 15 atm

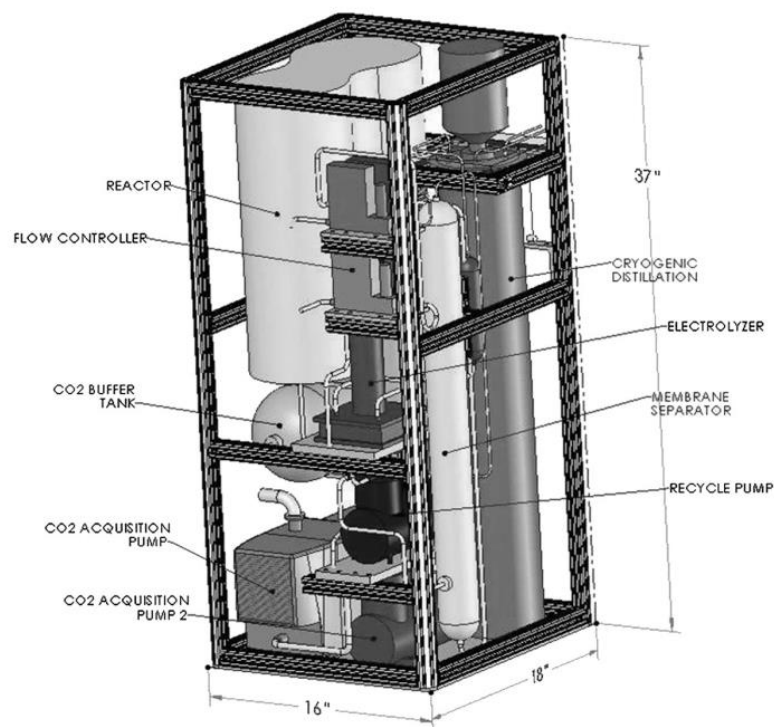
or high H<sub>2</sub> to CO<sub>2</sub> ratios) [16], the conversion rate of the reaction is substantially lower than the Sabatier process [8] meaning that there is a need for a hydrogen recirculation loop that makes the system complicated (see Fig 1.4). RWGS, like the Sabatier process, requires a hydrogen input to create oxygen.



**Figure 1.4.** Scheme of an RWGS/Electrolysis process for oxygen production on Mars [14].

In the case of both processes, a considerable amount of power is needed to heat the reactor system to a high temperature (400 °C) and to compress CO<sub>2</sub> to high pressures. The sorption pump technology was used for older ISRU projects such as the Mars 2001 Surveyor Lander [17]. These work by absorbing and collecting CO<sub>2</sub> during night-time on Mars via passive cooling, then passively or electrically heating the sorbent and releasing the gas at high pressure [18]. They have a minimal energy need (the only energy demand is for heating the bed for desorption), but they require huge tanks of the adsorbent (often zeolite) to store the CO<sub>2</sub>. Cryogenic storage is also based on a cyclical work pattern in which a cold point is required to collect CO<sub>2</sub> as a solid that can subsequently be heated up as needed. It takes up less space and mass but is inefficient in terms of energy [19]. The third alternative for achieving the needed pressures is to employ a mechanical compressor, which can operate in a flow-through configuration (that eliminates the requirement for

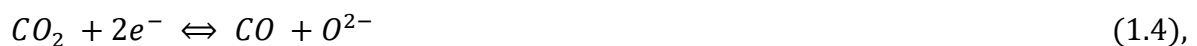
high-pressure storage) and takes significantly less space, but also relatively higher power is needed. However, its power requirement is still lower than the cryogenic pump [20][21]. **The Integrated Mars In Situ Propellant Production System (IMISPPS)** is the most optimized Sabatier/RWGS-based system, which is designed to create a combination of CH<sub>4</sub> and O<sub>2</sub> at 100 per cent conversion for use as a propellant [20]. The IMISPPS makes use of both the Sabatier and RWGS processes with a recycle loop to achieve an 18 to 1 leverage ratio (1 kg of hydrogen needed to produce 18 kg of propellant). At the same time, it can produce 1 kg of propellant (two-thirds being oxygen) during 24 hours using 700 W of power.



**Figure 1.5.** CAD drawing of the IMISPPS [21]

### 1.2.3 Solid oxide electrolysis

Another method of splitting CO<sub>2</sub> for oxygen production technology is called the Solid Oxide Electrolysis (shortly SOE), in which the following cathode reaction (solid oxide electrolysis of CO<sub>2</sub>) takes place:



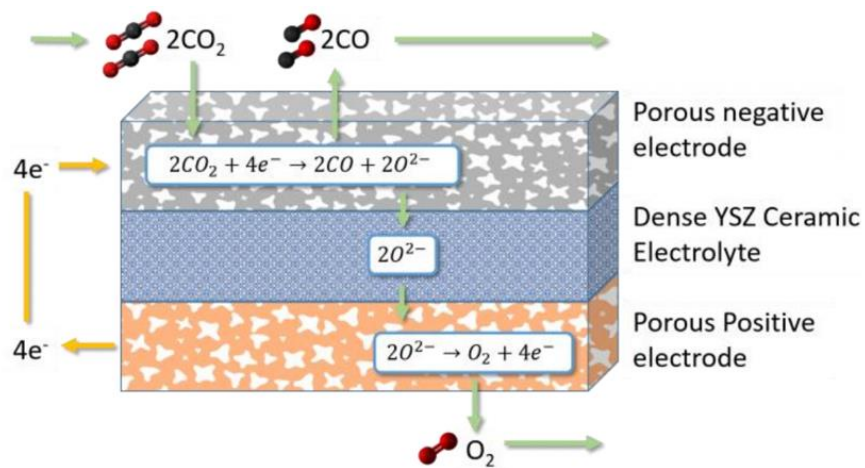


**Figure 1.6** Reactions across a SOXE cell

Here, carbon monoxide and the unused carbon dioxide are vented from the system while the oxide anions are delivered to the anode through a solid ceramic electrolyte, where gaseous oxygen is produced from their combination:



Being the most mature among the  $\text{O}_2$  production systems on Mars, SOE technology is the only field-tested alternative as well. Currently, the *Perseverance* rover sent to Mars for exploration employs OxEon Energy's SOE technology for oxygen production in the Jezero crater as part of the Mars Oxygen In-Situ Resource Utilization Experiment (MOXIE, Figure 1.7).

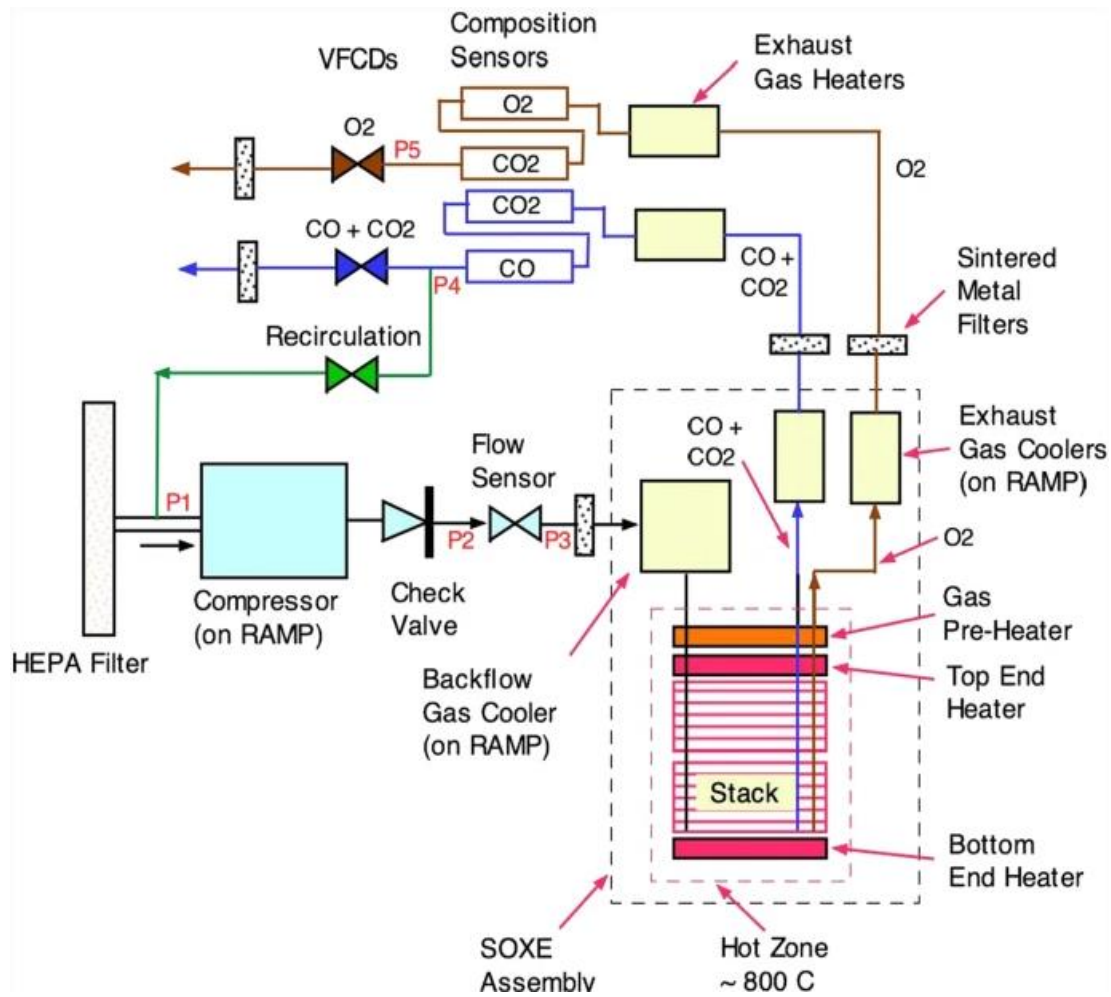


**Figure 1.7** Schematic representation of the MOXIE.

MOXIE captures Mars's atmospheric gas through a HEPA filter with a scroll compressor to compress it to 530-800 mbar and then reach its working temperature (800 °C) with an Inconel heat exchanger prior to the SOE stage. Dr Robert Ash was the first to introduce the SOE module now used in MOXIE for oxygen production in the 1970s, but this was not given enough attention (it was dismissed as "major advances above already shown levels of performance may be viewed as very improbable" in 1997) until 2013 when NASA chose MOXIE from its Announcement of Opportunity for ISRU technologies. A scandia-doped zirconia ceramic oxygen-conducting membrane, a doped lanthanum cobalt ferrite oxygen evolution electrode (anode), and a nickel-ceria cermet CO/CO<sub>2</sub> electrode (cathode) designed particularly for MOXIE form the basis of the SOE module [21]. MOXIE is made up of 10 SOE cells, each of which converts 30-50 per cent of CO<sub>2</sub> into CO and O<sub>2</sub>. The gases are excited through oxygen, CO, and CO<sub>2</sub> sensors, with the anode stream being vented (though it would be collected in a full-scale experiment) and the cathode stream being recirculated into the SOE stack. With the output of 5.37 g h<sup>-1</sup> during its first test on

April 20, 2021, MOXIE has already proven itself, even though the theoretical maximum production rate is  $12 \text{ g h}^{-1}$  at 4A (limited by the power supply). The benefits of the SOE technology include its evident high space TRL, system simplicity, relatively low input pressure (as compared to Sabatier/RWGS processes), and the fact there is no need for hydrogen. However, the downsides include the high working temperature (which makes the power demand of the module very high), the ceramic components' (thermal and mechanical) fragility, the limiting reaction of carbon production (which, as it happens, forms the basis for the MSCC-ET system) and the large surface area necessary to conduct the reaction at a reasonable rate.

Table 1.1 shows a comparison of the existing Mars ISRU technologies for oxygen generation. It is obvious that all of the systems produce oxygen at around the same rate, while the combined Sabatier-RWGS system is the most efficient limited by its higher mass budget. The Sabatier/electrolysis and RWGS/electrolysis systems were estimated to be the lightest among all, although this is not experimental evidence from a real system. Considering the mass of elements from the IMISPPS system (that has both RWGS and Sabatier modules), the true weight might be up to 2-3 times higher than the minimum weight stated in the Table.

**Table 1.1** Comparison of Mars ISRU technologies.

<b>Technology</b>	Reactants	Products	Working temperature (°C)	Working pressure (bar)	Oxygen production rate (g kWh <sup>-1</sup> )	System mass (kg)**
<b>Sabatier</b>	CO <sub>2</sub> , H <sub>2</sub>	O <sub>2</sub> , CH <sub>4</sub> , H <sub>2</sub>	>400	>15	54.1	33
<b>RWGS</b>	CO <sub>2</sub> , H <sub>2</sub>	O <sub>2</sub> , CO, H <sub>2</sub>	400	10	49.4	37.5
<b>IMISPPS</b>	CO <sub>2</sub> , H <sub>2</sub>	O <sub>2</sub> , CH <sub>4</sub>	400	5	61.1	127.7
<b>SOE (MOXIE)</b>	CO <sub>2</sub>	O <sub>2</sub> , CO	800	1	54.7	71.2
<b>MSCC-ET</b>	CO <sub>2</sub>	O <sub>2</sub> , C	450-800	Under study	Under study	Under study

## 1.3 MSCC-ET AS A PROMISING TECHNOLOGY

### 1.3.1 Fundamentals of Molten salt CO<sub>2</sub> capture and electrochemical transformation (MSCC-ET)

The continued rise in CO<sub>2</sub> levels in the atmosphere has sparked widespread alarm about the impact of global climate change. CO<sub>2</sub>, the most well-known greenhouse gas, has been demonstrated to elevate the surface earth temperature by 4 degrees Celsius [22] when its quantity is doubled in the atmosphere. Climate change, rising sea levels, and the loss of numerous species will become more visible in the coming decades if no regulatory measures are implemented [23].

CO<sub>2</sub>, on the other hand, is a valuable carbon resource that is used to make urea, salicylic acid, carbamates, and inorganic chemicals [24]. Environmentally friendly carbon materials are a crucial support for strategic new sectors, with large market potential. As a result, turning CO<sub>2</sub> into valuable products like hydrocarbons and other compounds, in addition to CO<sub>2</sub> capture and storage (CCS), is extremely desirable for sustainable growth [25][26]. Due to the reduced load on limited geological storage sites in CCS operations, carbon capture, utilisation, and storage (CCUS) are especially appealing as a midterm option [27] [28]. That is why CO<sub>2</sub> capture and storage and also the conversion of CO<sub>2</sub> to other functional materials (such as carbon and oxygen) are among the pathways to a sustainable future. It has the ability to contribute to the earth's atmospheric carbon balance, intermittent renewable energy storage, carbon materials manufacturing, and local environment air quality control.

MSCC-ET is among the most promising CO<sub>2</sub> capturing technologies. Molten salt carbon capture and electrochemical transformation (MSCC-ET) is a technology that converts CO<sub>2</sub> into value-added carbonaceous products and oxygen through electroreduction of CO<sub>2</sub> in molten salts. Carbon is the favored product when Li<sub>2</sub>CO<sub>3</sub> and/or CaCO<sub>3</sub> are present in molten salts, according to the data in Table 1 and tests conducted by several groups [29]. As a result, CO<sub>2</sub> can be absorbed and degraded in high-temperature molten salts using Li<sub>2</sub>CO<sub>3</sub> and/or CaCO<sub>3</sub>, forming the basis for the molten salt CO<sub>2</sub> capture and electrochemical transformation (MSCC-ET) process.

**Table 1.2.** The equilibrium activity of corresponding metal oxide and the deposition potential of metals (EM) and carbon (EC) in different molten carbonates at 450 C under a CO<sub>2</sub> atmosphere of 1.0 atm

Molten salt	Activity of $M_xO^a$	$E_M/V$ vs. $CO_2-O_2/CO_3^{-2}$	$E_C/V$ vs. $CO_2-O_2/CO_3^{-2}$
$Li_2CO_3$	$1.04 \times 10^{-821}$	-3.183	-1.883
$Na_2CO_3$	$2.46 \times 10^{-16}$	-2.757	-2.681
$K_2CO_3$	$2.05 \times 10^{-21}$	-2.829	-3.251
$CaCO_3$	$2.31 \times 10^{-521}$	-3.230	-1.523

Carbon (in the form of carbon powder, film, or metal complexes) and/or carbon monoxide are the most common results of electrochemical transformation from  $CO_2$  in high-temperature molten salts, depending on the temperature and applied cell voltage [30][31].

Molten salt used as an electrolyte is essential for capturing  $CO_2$ , transporting reactants and ions, and maintaining the cell's temperature balance. MSCC-ET is made up of three processes:

- $CO_2$  is absorbed by molten salt
- electrochemical reactions on the cathode and anode
- products separation and collection

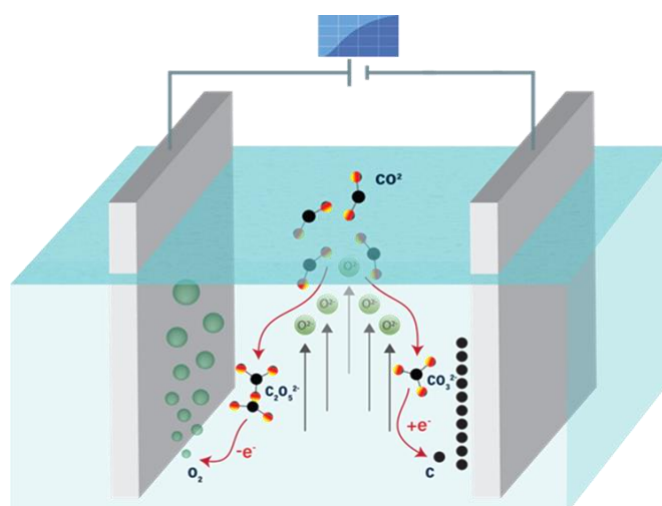


**Figure 1.8.** Schematic representation of the MSCC-ET process.

The advantages of inorganic molten salts are extensive. First of all, molten alkali carbonate salts have a wide potential window. Secondly, the CO<sub>2</sub> conversion rate of high-temperature molten salts is higher than low-temperature electrolytes due to the faster diffusion of electroactive ions and electrode reactions. Other advantages of inorganic molten salts include the relative simplicity of the process (meaning that a complicated cell is not needed) and a low overpotential, meaning that it does not require a catalyst.

The amount of carbon that can be extracted from the process depends mainly on the duration of the synthesis and the reaction conditions (pressure, CO<sub>2</sub> flow, potential, current density, etc). Thus, the molten salt composition affects both CO<sub>2</sub> absorption and electrochemical reaction processes due to the different physicochemical features of molten salts such as basicity, solubility, viscosity, and so on. In the case of the carbonate salts, the basicity can be expressed as the tendency to donate oxide ions, which is important as the absorption rate of CO<sub>2</sub> increases when metal oxides with strong basicity are used [29]. For example, the basicity of three metal carbonates is expressed as follows: Li<sub>2</sub>CO<sub>3</sub> > Na<sub>2</sub>CO<sub>3</sub> > K<sub>2</sub>CO<sub>3</sub> [32]. Thus, by increasing the amount of Li<sub>2</sub>CO<sub>2</sub> in the mixture, the overall basicity of the salts can be controlled. At the same time, increasing the reaction temperature has been suggested as a pathway to reduce the viscosity of carbonate salts [33]. The production of oxygen during the reaction is another important advantage. In general, research on MSCC-ET is primarily focused on two aspects. One of them is optimizing the particle size, morphology and specific surface area of the produced carbon so that it can better suit the desired application in different fields and the other is to find inert anode materials for the oxygen formation.

### 1.3.2. CO<sub>2</sub> capturing mechanism of the MSCC-ET process

Carbon and O<sub>2</sub> are the CO<sub>2</sub>-splitting products on the cathode and anode, respectively, in the MSCC-ET process. The possible reactions in an MSCC-ET reactor are the following [29]: (1.6)-(1.9)





Here, the carbonate is reduced to carbon (eq (1.6) and (1.7)) or carbon monoxide (eq (1.6a) and (1.7a)) in molten salts containing  $M_xCO_3$  ( $M = Li, Ca, \text{etc.}$ ) while metal oxide and oxygen are released. The difference between equation (1.6) and equation (1.7) originates from the anodic reaction. The generated carbon monoxide can be further reduced to carbon (equation (1.8)) depending on the experimental parameters. At the same time, the formed oxide absorbs  $CO_2$  and reproduces the carbonate salt (equation (1.9)) which ensures that the process remains sustainable. The molten salt used to produce carbon from  $CO_2$  must be capable of dissolving oxygen ions so that  $CO_2$  can be absorbed and transformed into carbonate ions.

The  $CO_2$  absorption equilibrium amount for each molten salt shows the amount of  $CO_2$  that can be captured by using the given salt as electrolyte [32]. In this process, the most commonly used salts are  $Li_2CO_3$ ,  $Na_2CO_3$  and  $K_2CO_3$  and their mixtures. In addition to  $Li_2CO_3$ ,  $Na_2CO_3$  and  $K_2CO_3$ ,  $Li_2O$ ,  $Na_2O$  and  $K_2O$  also exist in the mixture (as expressed by the absorption equilibrium in eq (1.9)). In the case of molten  $Li_2CO_3$ , the thermodynamically preferred deposition is of carbon rather than Li at  $600^\circ C$  [32]. However, in  $Na_2CO_3$  and  $K_2CO_3$ , the thermodynamically preferred deposition component is the metal. That is why  $Li_2CO_3$  is considered an important part of metal carbonates for the purpose of carbon deposition. As the energy of decomposition for  $Na_2O$  and  $K_2O$  is lower than  $Li_2O$ , they are more likely to decompose during the reaction instead of leading to carbon deposition. To sum up, molten salts containing  $Li_2CO_3$  are much better candidates for carbon deposition.

## 1.4 MSCC-ET for Mars exploration

NASA's Mars Oxygen In-Situ Resource Utilization Experiment has already demonstrated some promising attempts at extracting oxygen from the Martian atmosphere for use as propellant and breathing. MOXIE separates oxygen atoms from carbon dioxide molecules (one carbon atom and two oxygen atoms). Carbon monoxide, a waste product, is released

into Mars' atmosphere [1]. Whereas the MSCC-ET process does not release carbon monoxide as a byproduct instead different types of carbon materials are produced. This means that on top of the produced oxygen that can be used for breathing, the carbon materials can be used in a variety of applications like energy storage (battery and ultracapacitor technologies), energy production (fuel cell) and other fields (conductive and strengthening coatings, polymer formulations and water filters).

Although there are many advantages of the technology, certain limitations exist that need to be solved. These include questions such as:

- What is the efficiency of solid carbon storage and reoxidation in the Martian atmosphere at a voltage that solar panels might produce?
- How pure are the gaseous oxygen products produced in such a reactor, and can they be utilized to regenerate artificial air?
- Whether the relatively high temperatures required to melt the electrolytes in a small reaction can be achieved in Mars conditions?
- How does the solubility of CO<sub>2</sub> change depend on different electrolytes? Because it impacts the electrolyte's electrical conductivity, current efficiency during the electrolysis process, and electrode processes [34]
- How much electrolyte weight is lost during carbonate reproduction and C/O production stages?

Certainly, all of these points require detailed research to find answers and to make the MSCC-ET process the most efficient option for Mars exploration. In terms of practicality, it is especially important to evaluate the stability of different carbonate salt mixtures in Mars conditions and analyze the produced carbon materials. As long-term operation under harsh conditions is part of exploration missions, the stability of the chosen electrolyte can influence the performance of the whole technology and a better understanding of the process can be very useful for making a good choice. In addition, carbon nanomaterials are commonly employed in fuel cells as a catalyst support material and the carbon from MSCC-ET can be used in the manufacturing of fuel cells for producing electricity on Mars. However, the fuel cell catalyst support material must satisfy several requirements such as resistance to corrosion, high conductivity, inertness, large surface area etc. That is why establishing a relationship between the properties of carbon material and the reaction conditions is a much-needed goal [35].

## **1.5 SUMMARY OF THE LITERATURE REVIEW AND AIM OF THE STUDY**

Due to increasing threats of climate change on the Earth, the topic of Mars exploration has received a lot of attention in recent years. The reason why Mars is the most suitable candidate for exploration and future colonization is that it is the second – the closest planet to us stands at roughly the same velocity and has around the same tilt angle, day length etc. At the same time, it might hold the answers to other questions about the origin and evolution of life on earth. However, key differences between the two planets make the terraforming of Mars a challenging task with various aspects such as scientific-technological, ethical and financial. Among these, the scientific-technological challenges may be the most demanding as it involves huge projects like warming the planet, changing its atmosphere, activating its hydrosphere and producing oxygen.

In the review, current oxygen and carbon production technologies (the Sabatier or Reverse Water-Gas Shift Reaction (RWGS), solid oxide electrolysis (SOE), and the MSCC-ET process) were discussed in detail and it was concluded that the MSCC-ET process is the most promising technology that can be used in Mars conditions due to its significant advantages over the other technologies. For example, the carbon output of this process can be utilized in a lot of applications ranging from energy storage (battery and ultracapacitor technologies) to energy production (like fuel cells).

The main limitation of MSCC-ET is that some details of the process are not well-known and wide research and development are required. One of these details is to understand the stability of electrolytes during all stages of carbon and oxygen production during Mars exploration.

In this work, the stability of three different eutectic salts ( $\text{Li}_2\text{CO}_3\text{-Na}_2\text{CO}_3\text{-K}_2\text{CO}_3$ ,  $\text{Li}_2\text{CO}_3\text{-Na}_2\text{CO}_3$ ,  $\text{Li}_2\text{CO}_3\text{-K}_2\text{CO}_3$ ) was analyzed in terms of weight loss when used as an electrolyte for MSCC-ET reactions. This was achieved by exposing each molten salt to 100% Ar gas flow (to imitate the reaction in case of  $\text{CO}_2$  absence) followed by a mixture of  $\text{CO}_2$ , Ar and  $\text{N}_2$  (Mars conditions) and lastly, by applying a voltage to start electrolysis again in the  $\text{CO}_2$ , Ar and  $\text{N}_2$  mix. The weights of eutectic salts were measured before and after each step to compare the amount of weight loss in the case of each salt. This was used to choose the best candidate that could be used in MSCC-ET for future Mars exploration missions.

## 2. EXPERIMENTAL

### 2.1 Preparation of eutectic mixtures

In this study, three different eutectic carbonate salt mixtures were prepared for the reaction. These were  $\text{Li}_2\text{CO}_3\text{-Na}_2\text{CO}_3\text{-K}_2\text{CO}_3$  (shortly as Li-Na-K carbonate),  $\text{Li}_2\text{CO}_3\text{-Na}_2\text{CO}_3$  (Li-Na carbonate) and  $\text{Li}_2\text{CO}_3\text{-K}_2\text{CO}_3$  (Li-K carbonate). The melting points, and molar and weight ratios of the salts are given in Table 2.1 below.

**Table 2.1.** The melting points, molar and weight ratios of the salts used in this work

Salt mixture	Melting point (C)	Molar ratio (%)	Weight ratio(g)
$\text{Li}_2\text{CO}_3\text{-Na}_2\text{CO}_3\text{-K}_2\text{CO}_3$	399	43.5:31.5:25.0	32.1:33.4:34.5
$\text{Li}_2\text{CO}_3\text{-Na}_2\text{CO}_3$	488	62.0:38.0	46.8:53.1
$\text{Li}_2\text{CO}_3\text{-K}_2\text{CO}_3$	496	53.0:47.0	45.0:54.9

The stock carbonate salts were  $\text{Li}_2\text{CO}_3$  (99%, from Alfa Aesar),  $\text{K}_2\text{CO}_3$  (99.3%) and  $\text{Na}_2\text{CO}_3$  (100%, from Lachner). First, the alumina ( $\text{Al}_2\text{O}_3$ ) crucible (see Fig.8) to be used in the reaction was cleaned with ethanol (Keemia Kaubandus), dried in an oven and its weight was measured. Then the mixtures prepared in a glass beaker with given weight ratios were transferred to the crucible. Next, the weight of the salts and the crucible together was measured and the crucible was put to the bottom of a custom stainless-steel 304 cylindrical reactor (see Fig 2.1).



**Figure 2.1.** Alumina crucible (a) and the stainless steel reactor (b) (1-main body of the reactor, 2- gas inlet/ outlet and 3- temperature controller)

Before starting the reaction, the temperature inside the reactor was increased to a higher level than the melting point to fully melt and age the salt mixture, and after melting the salt mixture, the temperature was decreased to the selected temperature for each mixture.

## 2.2 Simulation of Mars conditions for MSCC-ET process

To simulate the working conditions of the reactor on Mars, the experiments were undertaken in a controlled gas environment. In order to avoid airflow into the reactor, it was sealed off with a stainless steel lid with a designated gas outlet and inlet (see Fig 2.2) The lid was sealed using a high-temperature silicone centering ring and the outlet and inlet tubes were also sealed with high-temperature silicone.

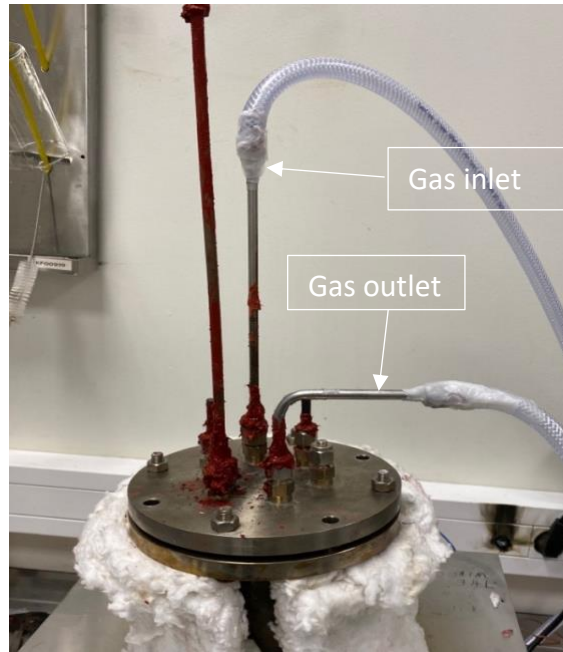


**Figure 2.2.** Reactor sealed with stainless steel lid and gas outlet/inlet. Red silicon sealant was used close small gaps.

After curing the silicone, a pump (IKA VACSTAR), inlet gas flow controllers (Alicat Scientific), gas outlet oxygen and temperature sensor (PyroScience GmbH) were connected to the reactor. The reaction was carried out in three steps as explained below:

1. The molten salt mixtures were kept at a relevant temperature for more than 8 hours exposed to 100% Ar flow and the pressure was maintained at 70 mbar. This was done to observe the stability of the mixture in the absence of  $\text{CO}_2$  (for example when the reactor is still in the spacecraft). Then the weight of the salt mixtures with the crucible was measured again to see how much weight loss occurred during this step
2. In the second step, the same procedure was repeated but under a mixture of  $\text{CO}_2$  (95%),  $\text{N}_2$ (3%) and Ar (2%) (to simulate the Martian atmosphere) from gas flow controllers and the weight of the crucible with salts were measured again
3. For the final part of the experiment, stainless steel 304 (due to its resistance to oxidation and low cost) cathode and anodes were inserted into the salt mixtures and the resistance of the electrolyte was measured with a multimeter to avoid short-circuit. After the voltage was applied to the electrodes for more than 8 hours to conduct an electrolysis reaction (see Fig 2.3) under simulated Martian atmosphere conditions. In the end, the cathode was checked to see if the reaction resulted in carbon formation and the crucible with salts was measured for the last time to conclude the experiment.

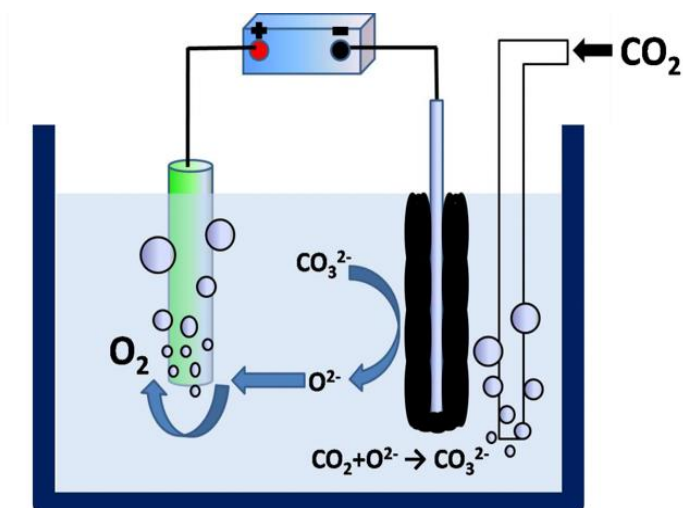


**Figure 2.3.** Schematic of electrolysis reaction under CO<sub>2</sub> flow [36]

To repeat the reactions with the same crucible, it was washed with 5M HCl to get rid of the salt residue (HCl reacts with carbonates to produce CO<sub>2</sub>), rinsed with ethanol and dried in an oven. In case of carbon formation in the cathode, it was immersed in 5M HCl solution, filtered, washed with deionized water and dried in an oven overnight.

### 2.2.1 Working principle of the oxygen sensor used in the experiment

The gas flow coming from the reactor was analysed with an oxygen sensor to quantify the amount of oxygen in the flow. This allows us to first establish a baseline and then measure the rate of oxygen generation during the electrolysis process. The oxygen monitoring was performed by an oxygen sensor (Pyroscience GmbH).

An optical oxygen sensor has two key components: an oxygen-sensitive sensor indication and a read-out device (oxygen meter). The oxygen meter is made up of an LED and a photodiode that stimulate and detect the oxygen-sensitive indicator's oxygen-dependent luminescence emission. Between the sensor indication and the oxygen meter, excitation and emission light are delivered over an optical cable.

The sensor layer's operating mechanism (see Fig 2.4) is based on the quenching of the special indicator (named REDFLASH) luminescence induced by oxygen molecules colliding with the indicator. This indicator is immobilized in a polymer matrix and may be coated directly onto optical fibres or transparent substrates fibre-optic sensors or contactless sensors. The oxygen meter modifies red excitation light sinusoidally, resulting in NIR near-

infrared) phase-shifted sinusoidally modulated emission. Because the sensor's emitted light is proportional to the oxygen partial pressure, it may be used to determine oxygen levels.

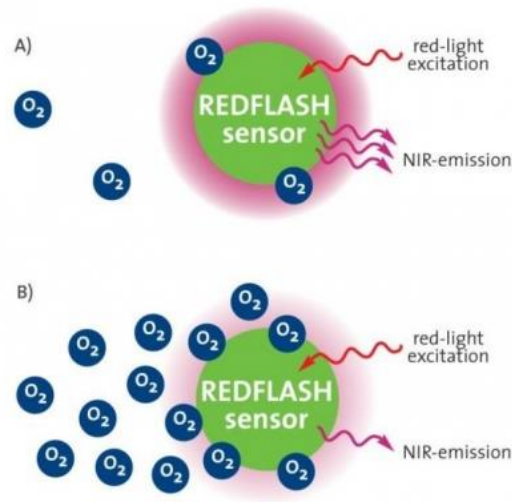


**Figure 2.4.** The operating mechanism of the oxygen sensor

### 2.2.2 X-ray Diffraction (XRD)

X-ray diffraction is a useful characterization technique for analyzing crystalline materials (materials with repetitive atomic positions). It is based on the interference between monochromatic X-rays and a crystalline sample that is measured. In a typical setup (see Fig 2.5), a cathode ray tube produces the X-rays, which are then filtered to create monochromatic radiation. Next, the radiation is concentrated and aimed onto the sample for measurement. When Bragg's Law ( $n\lambda=2d\sin\theta$ , where  $n$  is the order of reflection, the  $\lambda$  is wavelength of the radiation,  $d$  is the interplanar spacing and  $\theta$  is the incident angle between the x-rays and planes) is satisfied, constructive interference resulting from the interaction of incident rays with the material is created. The wavelength of electromagnetic radiation is associated with the diffraction angle and lattice spacing in a crystalline sample by this law. Due to the random orientation of the powdered material, scanning the sample across a range of  $2\theta$  angles should provide all potential lattice diffraction directions. The measured peaks are then allocated to reflection planes that describe the crystal structure of the material, and the peak values may also be used to estimate crystal size.

XRD measurements in this work were carried out with X'Pert3 Powder system by Malvern Panalytical by exposing the carbon material to 40 mA beam current and 45 kV beam voltage using Cu K $\alpha$  radiation ( $\lambda = 0.154$  nm).

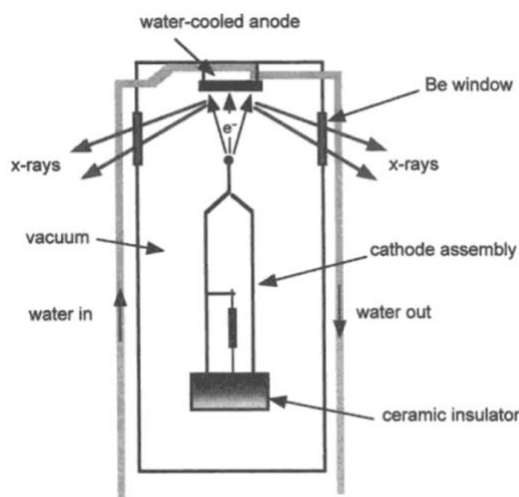


**Figure 2.5.** Schematic of a typical x-ray tube [37]

### 2.2.3 Scanning electron microscopy (SEM)

The scanning electron microscope (SEM) creates a wide range of signals at the surface of solid objects using a directed beam of high-energy electrons. The signals generated by electron-sample interactions provide information on the sample's morphology, its chemical composition, the orientation of the materials inside and its crystalline structure.

Usually, data is obtained across a specific region of the sample's surface, and a 2-d image is created. Using typical SEM imaging, areas in the width range of 1 centimetre to 5 microns may be studied in a scanning mode (magnification from 20X to about 30,000X with a resolution of 50 to 100 nm). The SEM can also be used to identify the chemical composition of the studied sample with energy-dispersive X-ray spectroscopy (EDX). In an SEM, accelerated electrons carry a lot of kinetic energy, that is dissipated as a different signal caused by electron-sample interactions as the incoming electrons decelerate in the solid sample. Secondary electrons (used to create SEM images), backscattered electrons (BSE), diffracted backscattered electrons (EBSD), photons, visible light and heat are among these signals. Secondary and backscattered electrons are both frequently employed for imaging: secondary electrons are good for displaying the morphology and topography of samples, while backscattered electrons are better for highlighting compositional differences in multiphase samples. The SEM (with EDX) measurement was

performed by Dr Valdek Mikli (Tallinn University of Technology) to reveal information about the structure and composition of the carbon material.

#### **2.2.4. Raman spectroscopy**

Raman spectroscopy is based on the Raman scattering of molecules, which expresses their vibrational, rotational, and other low-frequency modes. During the measurement, a sample is subjected to a powerful beam of monochromatic light (usually a laser beam) in the visible, near-infrared, or near-ultraviolet region frequency. Electromagnetic radiation can be transmitted, absorbed, or scattered when it interacts with a sample. When this monochromatic light is scattered by the molecules, the bulk of the radiation is scattered by Rayleigh scattering while a tiny percentage of the radiation has a frequency that differs slightly from the incident radiation. This phenomenon is called the Raman scattering or Raman effect and it is made up of several values of varying intensity and wavelength that correspond to molecular bond vibrations attributed to particular bonds, such as a carbon-carbon bond. By identifying these bonds in a given sample, it is possible to learn about the chemical structure, phase, polymorphism, intrinsic stress and strain of the material. As this is a non-destructive characterization method, the measured sample can be used in other applications as well. In this study, Horiba LabRam HR800 (with a 532 nm laser line) spectrometer with a spot size of 5  $\mu\text{m}$  diameter was employed and the measurement was performed at room temperature by Mehmet Ender Uslu from Tallinn University of Technology.

### 3. RESULTS AND DISCUSSION

#### 3.1 Stability of the studied eutectic salt mixtures in Mars conditions

In order to compare the stability profiles of salt mixtures (Li-Na-K carbonate, Li-K carbonate and Li-Na carbonate) under Mars conditions, the weight of the mixtures was measured prior to and after each step of the experiment. The observed weight loss of the mixtures given below can be used to make conclusions about the feasibility of the given mixture for use in Mars exploration missions as part of the MSCC-ET process:

**1. Weight loss in a neutral state (100% Ar flow) is shown as bar charts for each mixture:**



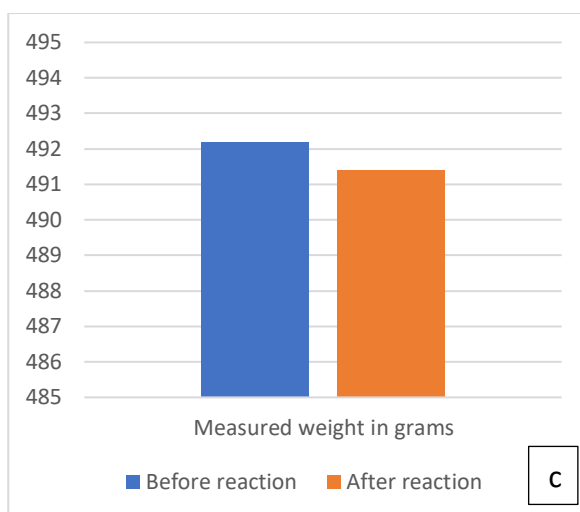


**Figure 3.1.** Weight loss comparison charts for a)  $\text{Li}_2\text{CO}_3\text{-Na}_2\text{CO}_3\text{-K}_2\text{CO}_3$ , b)  $\text{Li}_2\text{CO}_3\text{-K}_2\text{CO}_3$  and c)  $\text{Li}_2\text{CO}_3\text{-Na}_2\text{CO}_3$  mixtures (with crucible) in a neutral state without  $\text{CO}_2$  presence

While it is important to know about the stability of a given mixture in long-term working conditions, it is also essential to analyse the stability in case of a neutral state, for example when the reactor is still in the spacecraft and on the way to Mars. For this purpose, all three salt mixtures were exposed to Argon flow, heated to a high temperature and then left at the melting point for more than 8 hours. The weight of the mixtures with crucible was measured before and after the reaction as given in Figure 3.1. It can be seen that in comparison, Li-Na-K carbonate sample is the most stable in terms of weight loss as it lost about 0.64 grams while losses of Li-K carbonate and Li-Na carbonate were 0.68 and 0.79 respectively. However, there is not significant difference among all three carbonates under these conditions.

**2. Weight loss under a simulated Martian atmosphere ( $\text{CO}_2$ , Ar,  $\text{N}_2$ ) is shown as bar charts for each mixture:**

In the next stage, the conditions of the Martian atmosphere were simulated in the reactor and the mixtures were heated again to a higher temperature followed by a decrease in the melting temperature and exposed to a mixture of  $\text{CO}_2$ , Ar and  $\text{N}_2$  gases. The measured weight loss values showed that there is a bigger difference between the carbonates in contrast to the previous step. In Mars conditions weight loss of the Li-Na-K carbonate was the highest at 1.62 grams (see Fig 3.1a) and loss of Li-Na carbonate was 0.41 grams. However, Li-K carbonate was observed to be the most stable with a loss of only 0.22 grams.

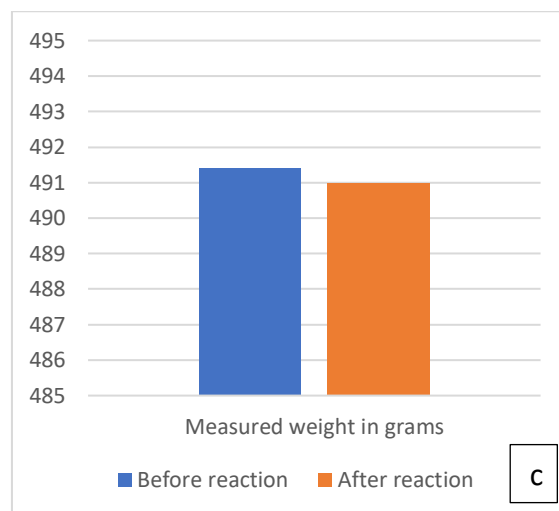
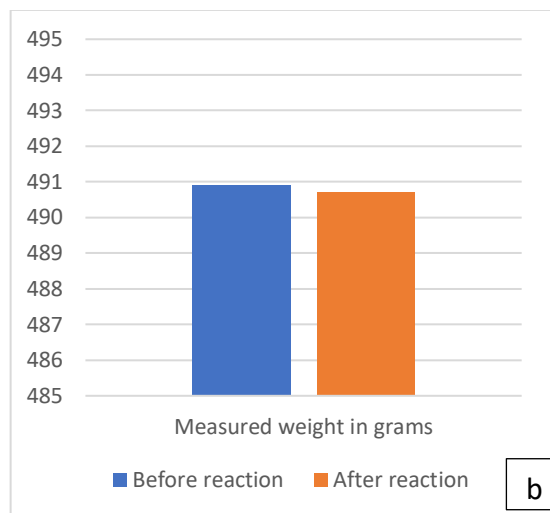


**Figure 3.2.** Weight loss comparison charts for a)  $\text{Li}_2\text{CO}_3\text{-Na}_2\text{CO}_3\text{-K}_2\text{CO}_3$ , b)  $\text{Li}_2\text{CO}_3\text{-K}_2\text{CO}_3$  and c)  $\text{Li}_2\text{CO}_3\text{-Na}_2\text{CO}_3$  mixtures (with crucible) under simulated Martian atmosphere ( $\text{CO}_2$ , Ar,  $\text{N}_2$ )

### 3. **Weight loss during electrolysis under simulated Martian atmosphere (CO<sub>2</sub>, Ar, N<sub>2</sub>)**

Perhaps, the most challenging step of the experiment is the electrolysis in Mars conditions as simultaneous carbon and oxygen production occurs and the reaction becomes more complex in this part. In this step, electrodes were inserted into the carbonates and the reaction was carried out in the same Mars conditions of the previous step. After the electrolysis, it was revealed that Li-Na-K carbonate lost about 0.24 g of its weight and the weight loss of Li-K carbonate and Li-Na carbonate were 0.27 g and 0.5 g (see Fig 3.3). At the same time, carbon was accumulated in the cathode in the case of Li-K carbonate and Li-Na carbonate while this was not the case for Li-Na-K carbonate. This might be due to several reasons such as incomplete electrolysis and experimental errors. The carbon produced from electrolysis in Li-K carbonate was taken from the electrode for characterization studies.



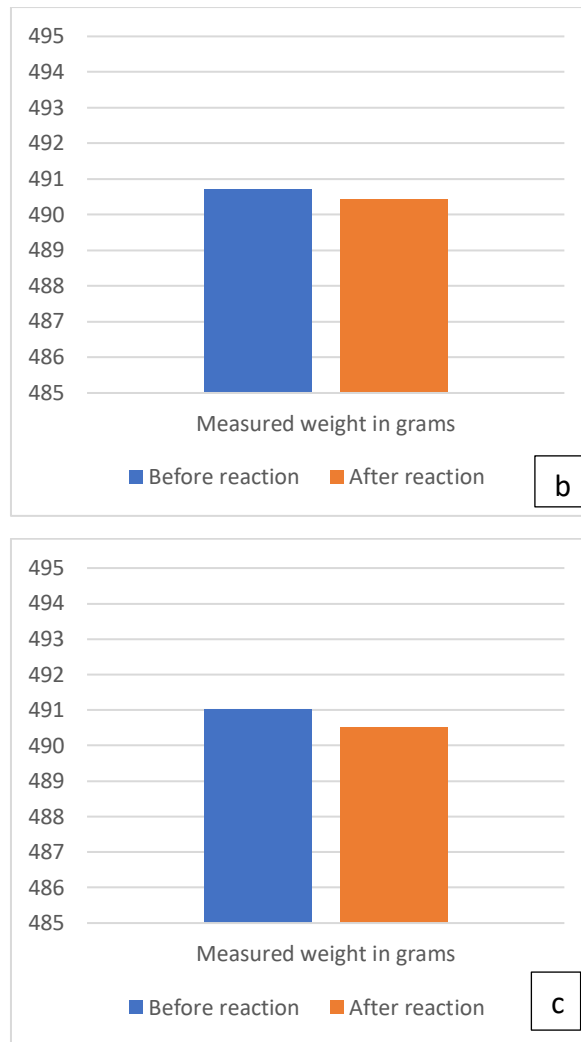


**Figure 3.3.** Weight loss comparison charts for a)  $\text{Li}_2\text{CO}_3\text{-Na}_2\text{CO}_3\text{-K}_2\text{CO}_3$ , b)  $\text{Li}_2\text{CO}_3\text{-K}_2\text{CO}_3$  and c)  $\text{Li}_2\text{CO}_3\text{-Na}_2\text{CO}_3$  mixtures (with crucible) during electrolysis under simulated Martian atmosphere ( $\text{CO}_2$ , Ar,  $\text{N}_2$ )

#### 4. Decay rates

In the case of the experiments in a neutral state (under 100% Ar flow) and simulated Mars condition ( $\text{CO}_2$ ,  $\text{N}_2$ , Ar flow) the reaction time for each mixture was different. That is why the weight lost by each mixture per hour (decay rate) gives a better measure of the true weight loss of the electrolyte.

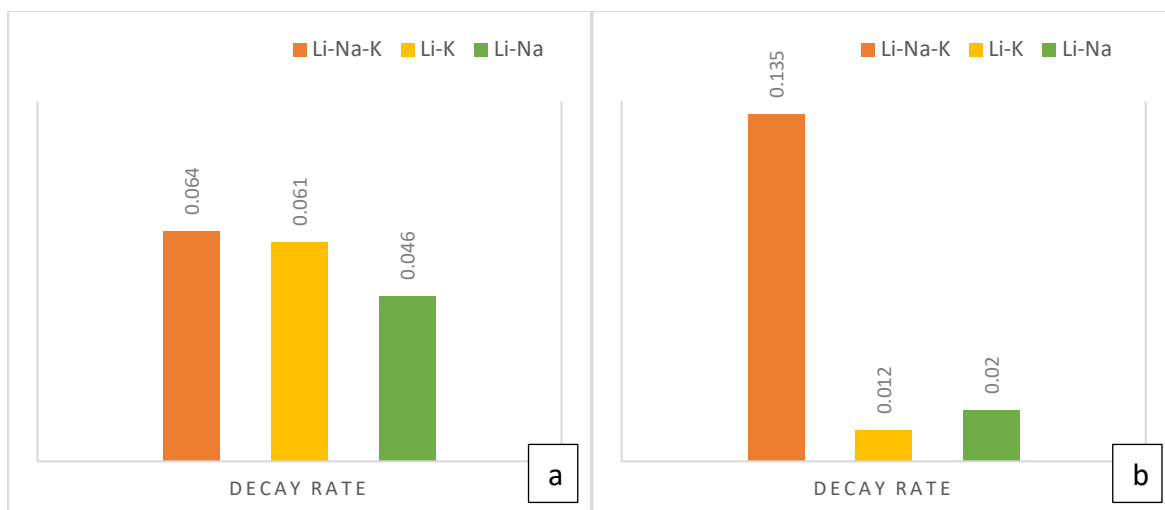


**Figure 3.4.** Overall decay rate comparison charts for Li<sub>2</sub>CO<sub>3</sub>-Na<sub>2</sub>CO<sub>3</sub>-K<sub>2</sub>CO<sub>3</sub>, Li<sub>2</sub>CO<sub>3</sub>-K<sub>2</sub>CO<sub>3</sub> and Li<sub>2</sub>CO<sub>3</sub>-Na<sub>2</sub>CO<sub>3</sub> mixtures in a) neutral state without the presence of CO<sub>2</sub> and b) under simulated Martian atmosphere (CO<sub>2</sub>, Ar, N<sub>2</sub>)

As we can see from Figure 3.4a the decay rate of Li-Na per hour (0.046 g·h<sup>-1</sup>) in a neutral state seems to be the lowest while this was not the case in Figure 3.4b. It is closely followed by Li-K mixture (0.061 g·h<sup>-1</sup>) and Li-Na-K experienced the highest decay rate per hour in this state. On the other hand, decay rate of Li-K was minimal (0.012 g·h<sup>-1</sup>) under Mars conditions and Li-Na-K mixture had a significant decay rate of 0.135 g·h<sup>-1</sup>. Li-Na mixture decay rate about 0.02 g·h<sup>-1</sup> which is slightly more when compared to Li-K.

In general, the average decay rate of Li-Na-K, Li-K and Li-Na carbonates in both conditions were 0.199 g·h<sup>-1</sup>, 0.073 g·h<sup>-1</sup> and 0.066 g·h<sup>-1</sup> respectively. While much lower decay rate were expected for the mixtures (due to the low surface area of the meniscus region observed on top of the electrolytes), such high decay rate might originate from different factors such as the presence of water in the crucible in the beginning, impurities of the electrolyte, experimental errors etc. In order to explain this high decay rate in detail, thermogravimetric analysis (TGA) can be performed to better observe the mass change of the mixture while the temperature is increased. This would provide information about the processes occurring inside the electrolyte at different temperature levels and show the exact reason behind this behaviour.

At the same time, carbon was obtained during electrolysis in Li-K (see Fig 3.5) and Li-Na-K carbonates, however as Li-K carbonate seems to be more stable, the carbon from Li-K will be characterized further.



**Figure 3.5.** Carbon produced from electrolysis in Li-K carbonate electrolyte on stainless-steel 304 electrode

## 3.2 XRD characterization

To study the crystallographic structure of the produced carbon sample (named as CO<sub>2</sub>-derived carbon or shortly CO<sub>2</sub>-C), it was analysed by XRD (see Fig 3.6). The distinctive peaks found in XRD were attributed to lithium chromium oxide (with reflection planes of [003] and [101], elemental chromium (reflection planes of [011] and [002]) and carbon with reflection plane of [200]. The broad peak at the Bragg angle of around 26° was related to the amorphous structure of the carbon while peaks at 18° and 37° were assigned to LiCrO<sub>2</sub> coming from the Li salt used in the reaction to produce carbon [38]. At the same time, the broadness of the peak at 26° could also be due to the contribution from the lithium carbide peak at 24°. The peaks of elemental chromium which is thought to be formed during the corrosion of stainless-steel electrodes were detected at angles of 44° and 64°.

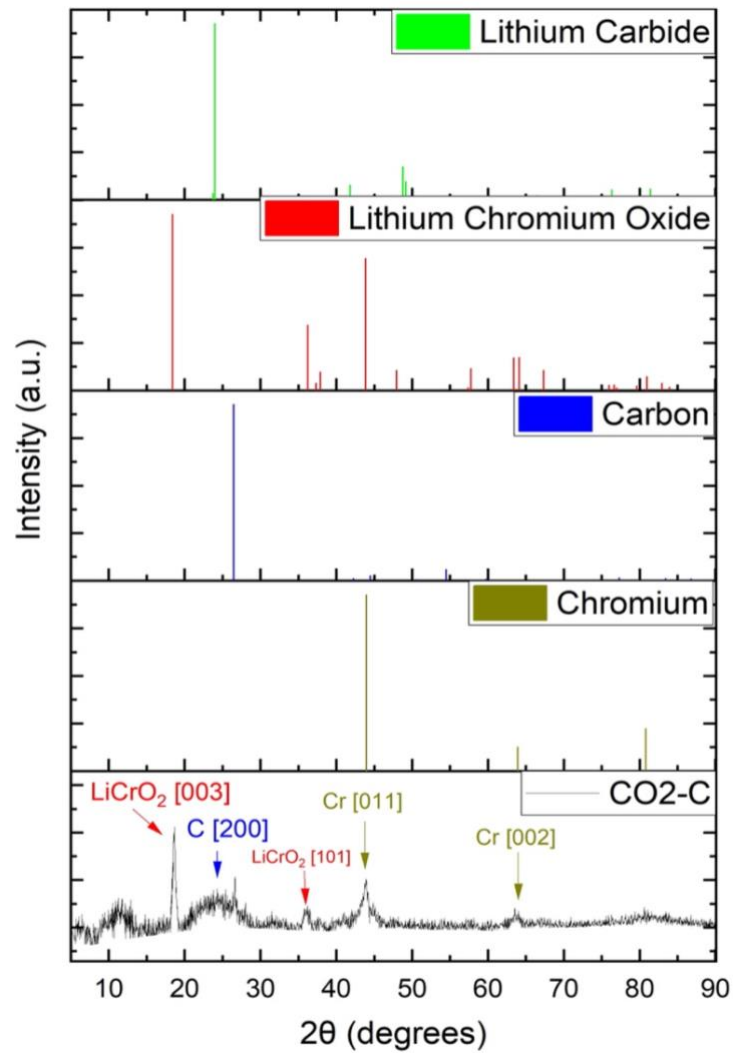


**Figure 3.6.** X-ray diffraction (XRD) patterns for lithium carbide, lithium chromium oxide, carbon, chromium and CO<sub>2</sub>-C (from top to bottom)

### 3.3 Raman spectra

To analyse the structure of the CO<sub>2</sub>-C material, Raman spectroscopy was performed (see Fig 3.7 ) The D-band and G-band are the two principal peaks (or bands) used to define Raman spectra of a measured sample. For CO<sub>2</sub>-C, only the first-order spectral range (from around 1000 to 2000 cm<sup>-1</sup>) was investigated and the associated D and G bands are displayed in Figure 3.7.

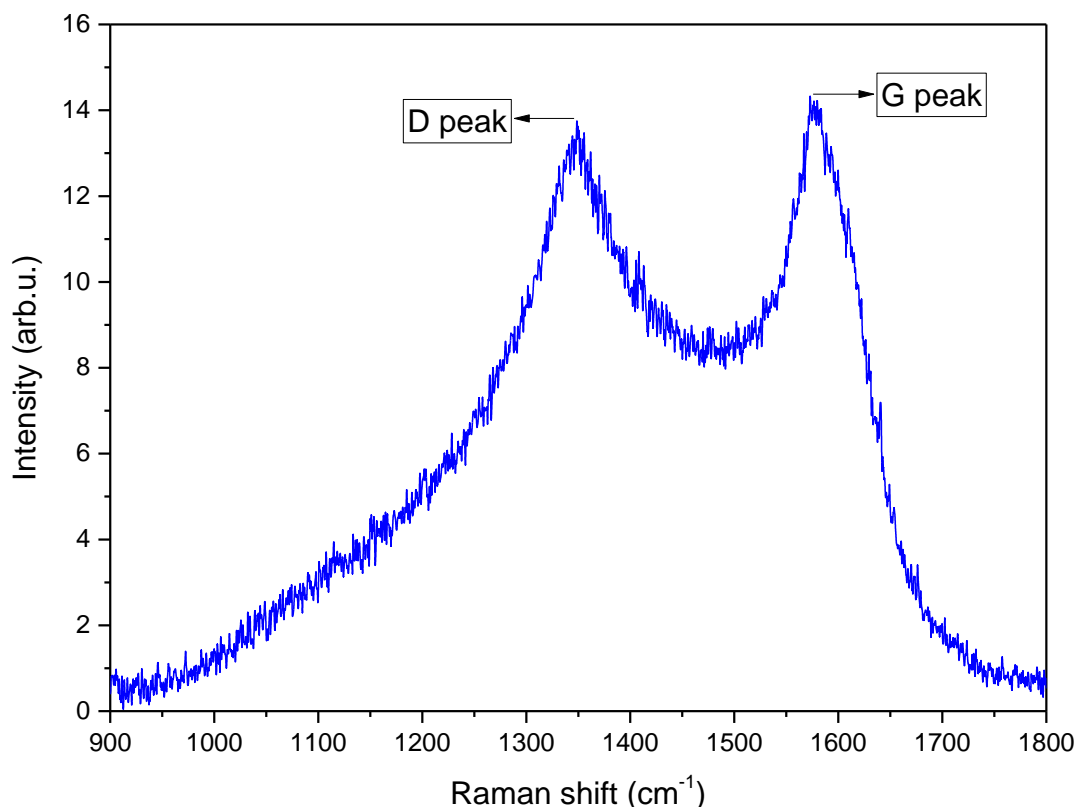


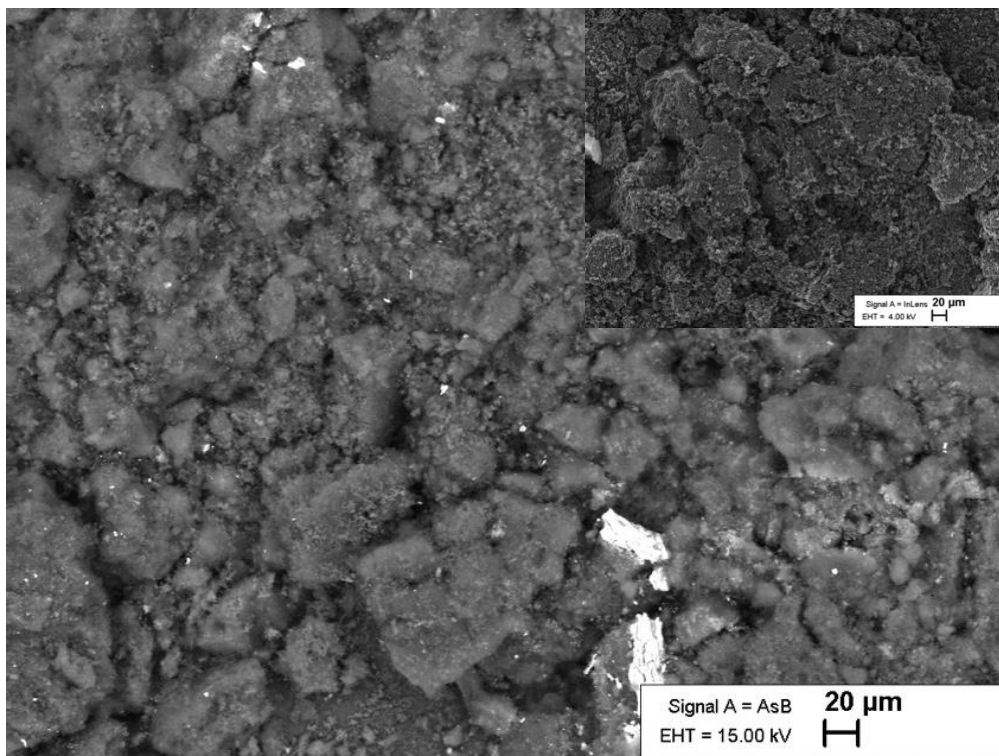
**Figure 3.7.** Raman spectra of CO<sub>2</sub>-C (532 nm laser line)

The Raman shift value for each peak may be used to learn about the physical features of the studied carbon material. The D-band, for instance, is formed by the edge of the ordered structures and the vicinity of defects, whereas the G-band is caused by the ordered graphite-like structures of the material [39]. By calculating the intensities of the D-band ( $I_D$ ) and the G-band ( $I_G$ ), it is possible to find the  $I_D/I_G$  ratio of the material which is commonly used to define the ordering and defective structure of the carbon materials [40]. Furthermore, in the case of disordered and/or partially graphitized carbons, other bands at around  $1150\text{ cm}^{-1}$ , at  $1450\text{ cm}^{-1}$  and  $1620\text{ cm}^{-1}$  can also provide relevant information.

The spectrum shows that the D and G-bands for CO<sub>2</sub>-C samples are about  $1350\text{ cm}^{-1}$  and  $1580\text{ cm}^{-1}$ . At the same time, the intensity of the peaks is 404 and 357 (in arbitrary units) for the D and G bands respectively giving the  $I_D/I_G$  ratio of 1.13. This might indicate and confirm again that the structure of the studied carbon material is amorphous and slightly disordered. It is worth to note that the disordered structure of the carbon has been linked to improved catalyst dispersion which in turn means improved catalyst efficiency for applications such as a fuel cell. [41]

### 3.4 SEM images (with EDX spectra)

The SEM and EDX measurements were performed to learn about the structure and composition of CO<sub>2</sub>-C. Based on the SEM images (see Fig 3.8) taken at different magnifications, it can be said that the carbon material is homogenous with varying particle size distribution. At the same time, it is possible to see both small and relatively bigger metal particles (brighter spots) that form agglomerates throughout the carbon.



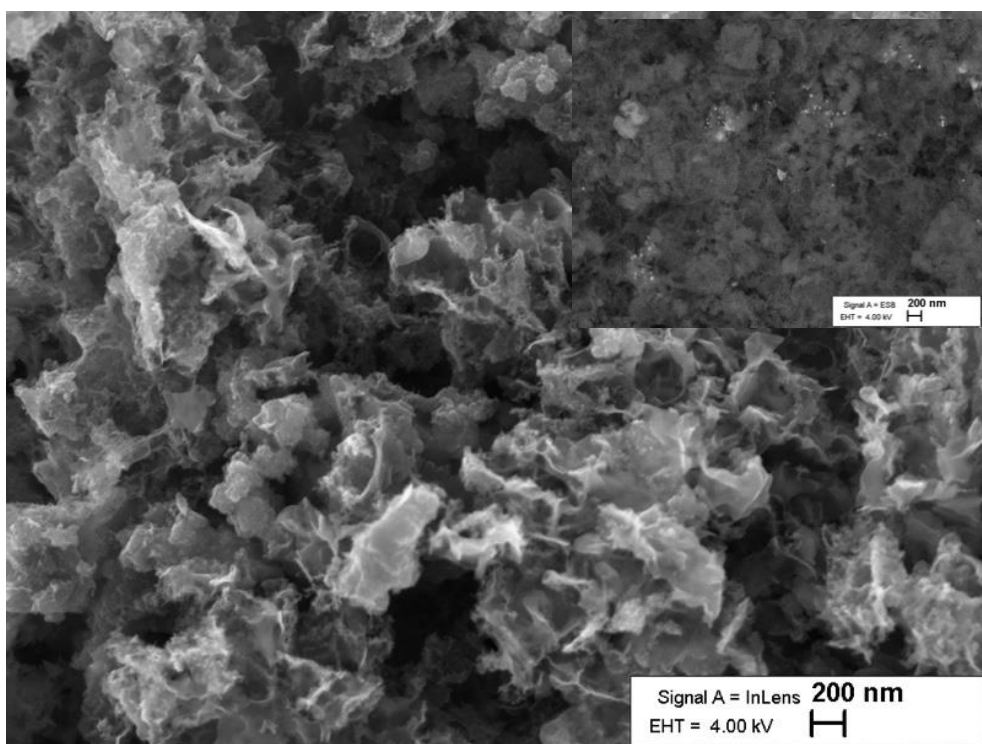


**Figure 3.8.** SEM images of CO<sub>2</sub>-C at different magnifications

The presence of metal particles was also confirmed in EDX spectrums taken from SEM images at 200  $\mu$ m magnification (see Fig 3.9).

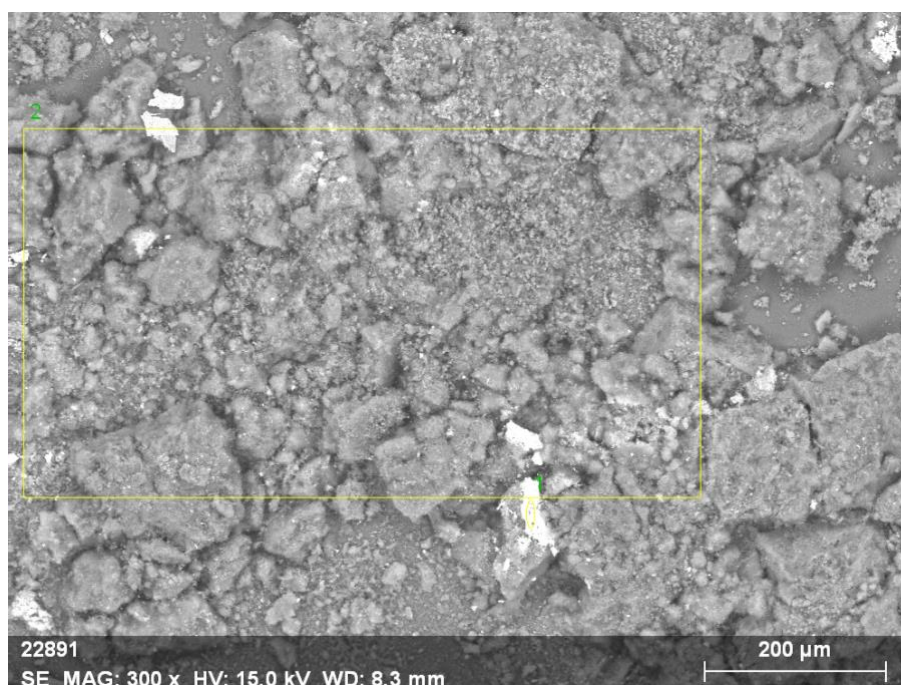


**Figure 3.9.** The areas of SEM image taken for EDX study (1-metal-rich area and 2-general area)

It was revealed that in the metal-rich area (see Fig 3.10) the sample contains about 40% chromium (see Table 3.1) which originates from the corrosion of stainless-steel electrodes used during electrolysis. This is in good agreement with the XRD results that indicated the presence of elemental chromium and lithium chromium oxide in the carbon. The traces of other substances in the carbon such as nickel, iron and silicon are also related to the electrode material while the source of carbon (CO<sub>2</sub>) can explain the oxygen found in the spectrum.

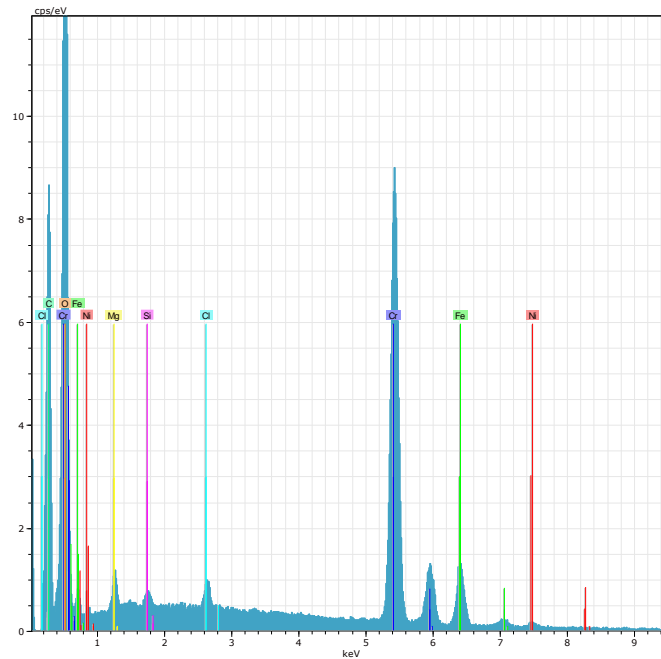


**Figure 3.10.** The EDX spectrum of the metal-rich area

**Table 3.1.** The concentration of elements in the EDX spectrum of the metal-rich area

Element	Series	unn. [wt.%]	C norm. [wt. %]	C Atom. [at.%]	C Error [%]
Nickel	K-series	1,37	1,47	0,60	0,1
Iron	K-series	9,25	9,96	4,25	0,3
Chromium	K-series	38,45	41,43	18,96	1,1
Chlorine	K-series	0,67	0,72	0,48	0,1
Silicon	K-series	0,35	0,37	0,32	0,0
Magnesium	K-series	0,98	1,06	1,04	0,1
Oxygen	K-series	27,77	29,92	44,51	3,6

Carbon	K-series	13,98	15,06	29,84	1,9
	Total:	92,80	100,00	100,00	

In the case of the EDX spectrum of the general area (see Fig 3.11), the composition included about 70% carbon (see table 3.2), followed by 28% oxygen and the rest being the metals observed in the metal-rich area.

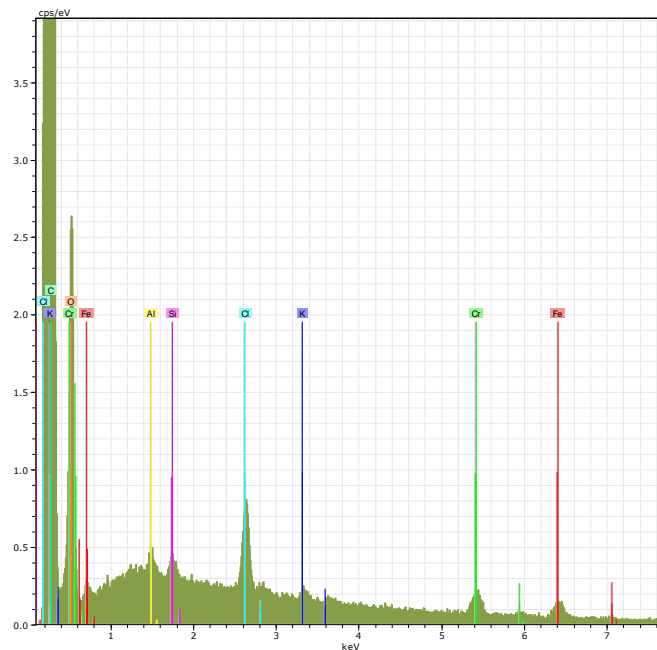


**Figure 3.11.** The EDX spectrum of the general area

**Table 3.2.** The concentration of elements in the EDX spectrum of the general area

Element	Series	Unn. [wt.%]	C norm. [wt.%]	C Atom. [at.%]	C Error [%]
Iron	K-series	0,98	0,98	0,23	0,1
Chromium	K-series	0,98	0,98	0,25	0,1
Potassium	K-series	0,15	0,15	0,05	0,0
Chlorine	K-series	0,81	0,81	0,30	0,1
Silicon	K-series	0,15	0,15	0,07	0,0
Aluminium	K-series	0,17	0,17	0,08	0,0

Oxygen	K-series	28,14	28,14	23,30	9,4
Carbon	K-series	68,63	68,63	75,71	22,5
	Total:	100,00	100,00	100,00	

## CONCLUSION

In this work, the stability of three carbonate mixtures ( $\text{Li}_2\text{CO}_3\text{-Na}_2\text{CO}_3\text{-K}_2\text{CO}_3$ ,  $\text{Li}_2\text{CO}_3\text{-Na}_2\text{CO}_3$  and  $\text{Li}_2\text{CO}_3\text{-K}_2\text{CO}_3$ ) was studied in terms of weight loss in three conditions for use in MSCC-ET reaction that makes it possible to capture and convert  $\text{CO}_2$  into valuable carbon nanomaterials. First, the mixtures were melted while exposed to Argon flow for several hours in order to quantify the weight loss in a neutral state (for example when the reaction takes place while the spacecraft is not in the Mars atmosphere). Next, the gas flow was changed to a mix of  $\text{CO}_2$ , Ar and  $\text{N}_2$  to imitate the Martian atmosphere and the reaction was carried out in this condition. Finally, electrodes were placed on each carbonate salt and electrolysis was started by applying a voltage to produce oxygen and carbon.

The weight of each electrolyte mixture was measured before and after the reactions to evaluate the stability of the given molten carbonate salt in 3 different scenarios. It was revealed that the average decay rate of Li-K and Li-Na carbonates were similar and lower than Li-Na-K carbonate. However, in general the average decay rates for the mixtures were higher than expected and this might be due to presence of water and impurities in the mixtures and experimental errors. In the future studies, the measurement with TGA is recommended to understand the processes leading to such high decay rates. Due to the fact that Li-K carbonate seems to be a promising candidate in terms of stability and it was also successful for the carbon production, the carbon sample produced from Li-K carbonate was taken for further characterization.

Characterization with X-ray diffraction showed that the structure of the studied carbon sample was largely amorphous and other distinctive peaks found were mainly attributed to lithium chromium oxide and elemental chromium present in the carbon. The sample was also analysed with Raman spectroscopy and it was again confirmed that the produced carbon material is mostly amorphous and its structure is slightly disordered with  $I_d/I_g$  ratio of 1.13. As disorder in carbon structure has previously been linked to improved catalyst dispersion (for fuel cell application, for instance), the disordered structure of the carbon material produced in this work can be considered advantageous.

To learn more about the structure of the produced carbon and its composition, SEM imaging with EDX analysis was performed. The SEM images at different magnifications demonstrated that the carbon material is homogenous but with certain metal particles were also detected in the image. This was later confirmed by the EDX spectrum as well. In the case of the metal-rich area of the material, the composition consisted of mostly chromium (around 40%) and traces of other substances such as nickel, iron and silicon. The presence of these elements was linked to the stainless-steel electrodes used in the

reactor during electrolysis. At the same time, the detected oxygen in the samples is thought to be originated from the source of the carbon which was carbon dioxide.

In conclusion, it can be noted that both  $\text{Li}_2\text{CO}_3\text{-Na}_2\text{CO}_3$  and  $\text{Li}_2\text{CO}_3\text{-K}_2\text{CO}_3$  mixtures were found to be promising candidates for MSCC-ET reaction in the Martian atmosphere owing to their superior stability in all of the studied conditions. As the carbon produced in the case of  $\text{Li}_2\text{CO}_3\text{-K}_2\text{CO}_3$  mixture was further analysed and found to be advantageous for use as a support material for fuel cell catalyst,  $\text{Li}_2\text{CO}_3\text{-K}_2\text{CO}_3$  can be the choice of electrolyte for future Mars exploration missions featuring MSCC-ET technology. Future studies may focus on optimizing this eutectic mixture even more to achieve better stability and carbon/oxygen production efficiency and perform TGA to understand the reason behind high decay rates in more detail.

## REFERENCES

- [1] EVAN ACKERMAN, "MOXIE Might Be the Most Exciting Thing Perseverance Has Brought to Mars," May 2021.
- [2] J. Hartvigsen, S. Elangovan, and F. Lyman, "MOXIE Development Driven Prospects for ISRU and Atmosphere Revitalization," *48th International Conference on Environmental Systems 8-12 July 2018, Albuquerque, New Mexico*.
- [3] R. B. Mathur, *Carbon nanomaterials: Synthesis, structure, properties and applications*. 2016. doi: 10.1201/9781315371849.
- [4] M. Beech, "Terraforming Mars: A Cabinet of Curiosities," in *Terraforming Mars*, 2021. doi: 10.1002/9781119761990.ch18.
- [5] Y. Xu, V. Ramanathan, and D. G. Victor, "Global warming will happen faster than we think," *Nature*, vol. 564, no. 7734. 2018. doi: 10.1038/d41586-018-07586-5.
- [6] G. Pezzella and A. Viviani, "Introductory Chapter: Mars Exploration - A Story Fifty Years Long," in *Mars Exploration - a Step Forward*, 2020. doi: 10.5772/intechopen.93448.
- [7] W. T. Huntress, V. I. Moroz, and I. L. Shevaley, "Lunar and planetary robotic exploration missions in the 20th Century," *Space Science Reviews*, vol. 107, no. 3–4. 2003. doi: 10.1023/A:1026172301375.
- [8] B. M. Jakosky and C. S. Edwards, "Inventory of CO<sub>2</sub> available for terraforming Mars," *Nature Astronomy*, vol. 2, no. 8, 2018, doi: 10.1038/s41550-018-0529-6.
- [9] L. P. Hinchman, "Long Ago and Far Away Requiem for Modern Politics: The Tragedy of the Enlightenment and the Challenge of the New Millennium . By William Ophuls The Case for Mars: The Plan to Settle the Red Planet and Why We Must . By Robert Zubrin and Richard Wagner ," *Polity*, vol. 31, no. 2, 1998, doi: 10.2307/3235232.
- [10] Gerald (Jerry) Sanders, "Current NASA Plans for Mars In Situ Resource Utilization," 2018.
- [11] D. Rapp, "Mars ISRU technology," in *Use of Extraterrestrial Resources for Human Space Missions to Moon or Mars*, 2013. doi: 10.1007/978-3-642-32762-9\_2.
- [12] D. Rapp, *Use of Extraterrestrial Resources for Human Space Missions to Moon or Mars*. 2018. doi: 10.1007/978-3-319-72694-6.
- [13] C. Vogt, M. Monai, G. J. Kramer, and B. M. Weckhuysen, "The renaissance of the Sabatier reaction and its applications on Earth and in space," *Nature Catalysis*, vol. 2, no. 3. 2019. doi: 10.1038/s41929-019-0244-4.
- [14] A. C. Muscatello and E. Santiago-Maldonado, "Mars In Situ Resource Utilization technology evaluation," 2012. doi: 10.2514/6.2012-360.

- [15] S. Pérez, J. J. Aragón, I. Peciña, and E. J. Garcia-Suarez, "Enhanced CO<sub>2</sub> Methanation by New Microstructured Reactor Concept and Design," *Topics in Catalysis*, vol. 62, no. 5–6, 2019, doi: 10.1007/s11244-019-01139-4.
- [16] R. Zubrin, M. B. Clapp, and T. Meyer, "New approaches for mars in-situ resource utilization based on the reverse water gas shift," 1997. doi: 10.2514/6.1997-895.
- [17] J. B. Sanders and D. I. Kaplan, "Mars ISPP precursor (MIP): The first flight demonstration of In-Situ propellant production," 1998. doi: 10.2514/6.1998-3306.
- [18] R. Zubrin, S. Price, L. Mason, and L. Clark, "An end-to end demonstration of a full scale mars sample return in-situ propellant production unit," 1995. doi: 10.2514/6.1995-2798.
- [19] A. Muscatello, R. Devor, and J. Captain, "Atmospheric Processing Module for Mars Propellant Production," 2014. doi: 10.1061/9780784479179.047.
- [20] R. M. Zubrin, A. C. Muscatello, and M. Berggren, "Integrated Mars In Situ Propellant Production System," *Journal of Aerospace Engineering*, vol. 26, no. 1, 2013, doi: 10.1061/(asce)as.1943-5525.0000201.
- [21] M. Hecht *et al.*, "Mars Oxygen ISRU Experiment (MOXIE)," *Space Science Reviews*, vol. 217, no. 1. 2021. doi: 10.1007/s11214-020-00782-8.
- [22] M. Johnson *et al.*, "Carbon nanotube wools made directly from CO<sub>2</sub> by molten electrolysis: Value driven pathways to carbon dioxide greenhouse gas mitigation," *Materials Today Energy*, vol. 5, 2017, doi: 10.1016/j.mtener.2017.07.003.
- [23] Z. Y. Zhao, R. D. Chang, and G. Zillante, "Challenges for China's energy conservation and emission reduction," *Energy Policy*, vol. 74, no. C, 2014, doi: 10.1016/j.enpol.2014.07.004.
- [24] I. A. Digdaya *et al.*, "Capture and conversion of CO<sub>2</sub> from oceanwater," *Nature Communications*, vol. 11, no. 2020, 2020.
- [25] G. Ibram, "Solar fuels vis-à-vis electricity generation from sunlight: The current state-of-the-art (a review)," *Renewable and Sustainable Energy Reviews*, vol. 44. 2015. doi: 10.1016/j.rser.2015.01.019.
- [26] B. Hu, C. Guild, and S. L. Suib, "Thermal, electrochemical, and photochemical conversion of CO<sub>2</sub> to fuels and value-added products," *Journal of CO<sub>2</sub> Utilization*, vol. 1. 2013. doi: 10.1016/j.jcou.2013.03.004.
- [27] D. T. Whipple and P. J. A. Kenis, "Prospects of CO<sub>2</sub> utilization via direct heterogeneous electrochemical reduction," *Journal of Physical Chemistry Letters*, vol. 1, no. 24, 2010, doi: 10.1021/jz1012627.
- [28] M. Aresta and A. Dibenedetto, "Utilisation of CO<sub>2</sub> as a chemical feedstock: Opportunities and challenges," *Journal of the Chemical Society. Dalton Transactions*, no. 28. 2007. doi: 10.1039/b700658f.

- [29] B. Deng *et al.*, "Molten salt CO<sub>2</sub> capture and electro-transformation (MSCC-ET) into capacitive carbon at medium temperature: Effect of the electrolyte composition," *Faraday Discussions*, vol. 190, 2016, doi: 10.1039/c5fd00234f.
- [30] D. Chery, V. Albin, V. Lair, and M. Cassir, "Thermodynamic and experimental approach of electrochemical reduction of CO<sub>2</sub> in molten carbonates", *International Journal of Hydrogen Energy*, 2014, vol. 39, no. 23. doi: 10.1016/j.ijhydene.2014.03.113.
- [31] D. Chery, V. Lair, and M. Cassir, "CO<sub>2</sub> electrochemical reduction into CO or C in molten carbonates: a thermodynamic point of view," *Electrochimica Acta*, vol. 160, Apr. 2015, doi: 10.1016/J.ELECTACTA.2015.01.216.
- [32] W. Weng, L. Tang, and W. Xiao, "Capture and electro-splitting of CO<sub>2</sub> in molten salts," *Journal of Energy Chemistry*, vol. 28. 2019. doi: 10.1016/j.jechem.2018.06.012.
- [33] M. Gao, B. Deng, Z. Chen, M. Tao, and D. Wang, "Enhanced kinetics of CO<sub>2</sub> electro-reduction on a hollow gas bubbling electrode in molten ternary carbonates," *Electrochemistry Communications*, vol. 100, Mar. 2019, doi: 10.1016/J.ELECOM.2019.01.026.
- [34] X. Hu, W. Deng, Z. Shi, Z. Wang, B. Gao, and Z. Wang, "Solubility of CO<sub>2</sub> in Molten Li<sub>2</sub>O-LiCl System: A Raman Spectroscopy Study," *Journal of Chemical and Engineering Data*, vol. 64, no. 1, 2019, doi: 10.1021/acs.jced.8b00722.
- [35] K. Kinoshita, "Carbon Materials. Carbon—Electrochemical and Physicochemical Properties. Wiley, New York 1988 " *Angewandte Chemie*, vol. 100, no. 9, 1988, doi: 10.1002/ange.19881000944.
- [36] M. Gao *et al.*, "(Invited) Electrochemical Deposition of Carbon Materials in Molten Salts," *ECS Transactions*, vol. 80, no. 10, 2017, doi: 10.1149/08010.0791ecst.
- [37] D. L. Dorset, "X-ray Diffraction: A Practical Approach," *Microscopy and Microanalysis*, vol. 4, no. 5, 1998, doi: 10.1017/S143192769800049X.
- [38] A. B. Siddique, A. K. Pramanick, S. Chatterjee, and M. Ray, "Amorphous Carbon Dots and their Remarkable Ability to Detect 2,4,6-Trinitrophenol," *Scientific Reports*, vol. 8, no. 1, 2018, doi: 10.1038/s41598-018-28021-9.
- [39] R. Härmas *et al.*, "Carbide-Derived Carbons: WAXS and Raman Spectra for Detailed Structural Analysis," *C (Basel)*, vol. 7, no. 1, 2021, doi: 10.3390/c7010029.
- [40] Tuinstra F and Koenig JL, "Raman Spectrum Of Graphite," *Journal of Chemical Physics*, vol. 53, no. 3, 1970, doi: 10.1063/1.1674108.
- [41] P. W. Albers, J. Pietsch, J. Krauter, and S. F. Parker, "Investigations of activated carbon catalyst supports from different natural sources," *Physical Chemistry Chemical Physics*, vol. 5, no. 9, 2003, doi: 10.1039/b212210n.